

Energy release patterns and shaking effects of earthquakes in the Japan Trench: A Hilbert-Huang Transform approach

Swapnil Mache¹ and Kusala Rajendran²

¹Indian Institute of Science

²Indian Institute of Science Faculty of Science

November 21, 2022

Abstract

Subduction zones showcase the multiplicity of earthquakes—interplate, intraplate and intraslab—with shallow, intermediate, or deep focus, associated with different energy release patterns and frequency contents. An understanding of the duration and frequencies associated with various pulses of energy is useful for damage assessment. Empirical Mode Decomposition (EMD) of strong-motion records and the application of Hilbert transform have been suggested to overcome the limitations of the Fourier spectral analysis in dealing with highly non-linear strong-motion records (Huang et al., 1998, Zhang et al., 2003). Following the same approach, we have been trying various methods of analysis using the KiK-net strong-motion records to explore the efficacy of these techniques in representing the source of the rupture, in terms of energy release and frequency distribution. Our previous studies used EMD and time-frequency analysis tools such as spectrogram, scalogram, and Hilbert spectrum, using Intrinsic Mode Functions (IMFs) of the original signals as inputs. Nishant (2019) made random picks of IMFs to represent sources by correlating the sum of the selected IMFs with the original signal but found that the results were station dependent. We selected IMFs based on their frequency content (0.1 to 3 Hz) and used their linear combinations to develop the Energy Release Functions (ERF) for individual earthquakes (Mache et al., 2019). They reported that the ability to capture the signature of the original signal using the IMFs varied between earthquakes and stations. Next, we selected stations based on the direction of rupture inferred from teleseismic waveform models. The use of appropriate combinations of individual IMFs, chosen based on the direction of slip, resulted in ERFs whose shapes compared better with the Moment Rate Functions (MRFs) obtained from the teleseismic models. To further explore the station dependence on the resolution of ERFs viz-a-viz the MRFs, we used the instrumental seismic intensity distribution maps (JMA 1996, Shabestari and Yamazaki 2001) to select the stations. We analyzed five earthquakes; two interplate (Mw 7.2 2005 Miyagi, and Mw 6.9 2008/07/19), two intraplate (Mw 7.0 2003 Sendai, and Mw 7.2 2012 Kamaishi) and one intraslab (Mw 7.1 2011 Miyagi), following the above methodologies. This abstract presents the initial results of our study, which to our knowledge, is the first of its kind and holds significant potential in understanding the spatial and temporal patterns of energy release and their associated frequencies. [cont.]



Energy release patterns and shaking effects of earthquakes in the Japan Trench: A Hilbert-Huang Transform approach

Swapnil Mache and Kusala Rajendran

Indian Institute of Science (IISc), Bangalore, India



1. Key Points

- 1. Specific Intrinsic Mode Functions (IMFs) represent energy release at the earthquake source.
- 2. Energy Rate Functions (ERFs) generated from Hilbert spectral analysis of such IMF combinations.
- 3. Proposed ERFs match well with the Moment Rate Functions (MRFs) from teleseismic waveform modeling.
- 4. ERF-MRF match is controlled by the station azimuth and shaking intensity, and frequency and energy-based selection of IMFs.

A short video explaining our work:

2. Motivation

- 1. Subduction zone earthquakes showcase different energy release patterns and frequency content depending on the **tectonic setting and depth**.
- 2. Interplate earthquakes, originating on the plate interface, show enhanced high-frequency energy (HFE) with increasing depth (Lay et al., 2012).
- 3. Outer-rise intraplate earthquakes produce enhanced HFE and ground shaking despite their high epicentral distances (Ye et al., 2013).
- 4. Intraslab earthquakes originate within the subduction slab (usually beneath population centers). They are more damaging than other similar Mw events due to enhanced HFE release and associated ground motion in a short duration, along with higher stress

3. Data

- 1. **Teleseismic data** from International Research Institutions for Seismology (IRIS). P and SH waveforms from 30-40 stations, epicentral distance 30° to 90°.
- 2. **Strong-motion acceleration data** from KiK-net, National Research Institute for Earth Science and Disaster Resilience (NIED, Japan). Data from the **vertical component of borehole sensors** (> 100 m depth) used in the analysis.

Event Number	Event Date (YYYY-MM-DD)	Event Time (hh:mm:ss.s)	Longitude (°E)	Latitude (°N)	Depth (km)	Mw	Tectonic Setting
1	2003-05-26	09:24:38.8	141.57	38.94	61.0	7.0	Intraslab
2	2011-04-07	14:32:50.6	141.85	38.32	53.3	7.1	Intraslab
3	2005-08-16	02:46:40.3	142.05	38.24	37.0	7.5	Interplate
4	2006-07-19	02:39:34.5	142.42	37.47	21.5	6.9	Interplate
5	2012-12-07	08:18:34.9	144.09	38.01	57.8	7.2	Intraplate
		08:18:46.9	143.83	37.77	19.5	7.2	Intraplate

Table: Earthquake details (from GCMT).

4. Methodology

Waveform inversion of teleseismic data

- 1. Kikuchi-Kanamori body-wave inversion program (Kikuchi and Kanamori, 1991) used for the analysis.
- 2. Moment Rate Function (MRF) generated from waveform modeling to validate the ERF algorithm.

Selection of strong-motion stations

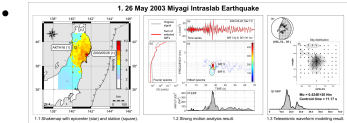
- 1. Slip distribution, along with the seismic intensity distribution maps (JMA, 1996; ShakeMap, 2017), used to select stations within the inferred azimuthal range and seismic intensity > 3.



5. Results

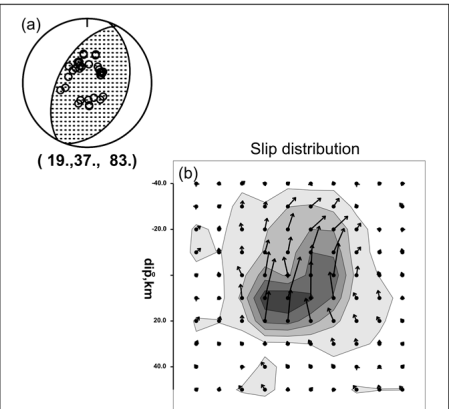
1. 26 May 2003 Miyagi Intraslab Earthquake (Mw 7.0, depth 67.0 km)

- Up-dip slip (towards east-northeast).
- Station AKTH16, WNW (305.98° azimuth), seismic intensity (SI) 4.
- Single, dominant, ~10 s energy pulse captured by both the ERF and MRF, along with a weaker tail.

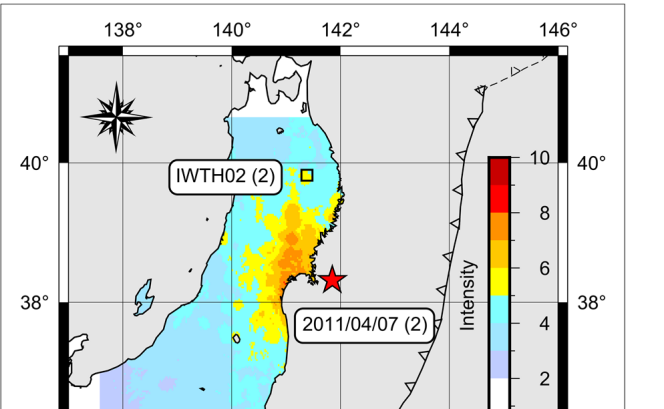


2. 07 April 2011 Miyagi Intraslab

Waveform Modeling



Strong motion station selection



6. Summary

- 1. HHT-based **ERF captures the earthquake source energy release**, with a **higher resolution** offered by HHT as compared to Fourier analysis methods and wavelet transform.
- 2. **ERF retains frequency information**, is computationally faster for a rapid interpretation of an event, and **does not entail assumptions** of the fault geometry and velocity structure. These are clear advantages over the traditional MRF.
- 3. **ERF captures complex ruptures** (2005 Miyagi-Oki event) and sub-events or multiple independent events (2012 Kamaishi event).

1. Key Points

1. Specific Intrinsic Mode Functions (IMFs) represent energy release at the earthquake source.
2. Energy Rate Functions (ERFs) generated from Hilbert spectral analysis of such IMF combinations.
3. Proposed ERFs match well with the Moment Rate Functions (MRFs) from teleseismic waveform modeling.
4. ERF-MRF match is controlled by the station azimuth and shaking intensity, and frequency and energy-based selection of IMFs.

A short video explaining our work:

4. Methodology

Waveform inversion of teleseismic data

1. Kikuchi-Kanamori body-wave inversion program (Kikuchi and Kanamori, 1991) used for the analysis.
2. Moment Rate Function (MRF) generated from waveform modeling to validate the ERF algorithm.

Selection of strong-motion stations

1. Slip distribution, along with the seismic intensity distribution maps (JMA, 1996; ShakeMap, 2017), used to select stations within the inferred azimuthal range and seismic intensity > 3.

6. Summary

1. HHT-based ERF captures the earthquake source energy release, with a **higher resolution** offered by HHT as compared to Fourier analysis methods and wavelet transform.
2. ERF retains frequency information, is computationally faster for a rapid interpretation of an event, and **does not entail assumptions** of the fault geometry and velocity structure. These are clear advantages over the traditional MRF.
3. ERF captures complex ruptures (2005 Miyagi-Oki event) and sub-events or

2. Motivation

1. Subduction zone earthquakes showcase different energy release patterns and frequency content depending on the **tectonic setting and depth**.
2. Interplate earthquakes, originating on the plate interface, show enhanced high-frequency energy (HFE) with increasing depth (Lay et al., 2012).
3. Outer-rise intraplate earthquakes produce enhanced HFE and ground shaking despite their high epicentral distances (Ye et al., 2013).
4. Intraslab earthquakes originate within the subduction slab (usually beneath population centers). They are more damaging than other similar Mw events due to enhanced HFE release and associated ground motion in a short duration, along with higher stress drop, increasing with depth (Choy et al., 2001; Okal and Kirby, 2002).
5. Conventional time-frequency analysis methods (Fourier transform, short-time Fourier transform, continuous wavelet transform) are deficient in resolving the above properties. They have a priori defined bases, are not suitable for nonlinear and nonstationary earthquake signals, and have limited resolution (Huang et al., 1998; Tary et al., 2014).
6. **Hilbert-Huang Transform (HHT)** overcomes these drawbacks

Energy release pa



Key Points

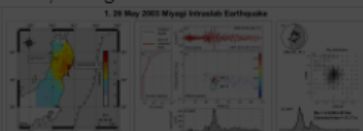
Specific Intrinsic Mode Functions (IMFs) represent energy release at the earthquake source. Energy Rate Functions (ERFs) generated from Hilbert spectral analysis of such IMF combinations. Proposed ERFs match well with the Moment Rate Functions (MRFs) from teleseismic waveform modeling. ERF-MRF match is controlled by the station azimuth and shaking intensity, and frequency and energy-based selection of IMFs.

Short video explaining our work

OPEN

Results

- 26 May 2003 Miyagi Intraslab Earthquake (Mw 7.0, depth 67.0 km)**
- Up-dip slip (towards east-northeast).
 - Station AKTH16, WNW (305.98° azimuth), seismic intensity (SI) 4.
 - Single, dominant, ~10 s energy pulse captured by both the ERF and MRF, along with a weaker tail.



n: A Hilbert-Huang



4. Methodology

Waveform inversion of teleseismic data

1. Kikuchi-Kanamori body-wave inversion program (Kikuchi and Kanamori, 1991) used for the analysis.
2. Moment Rate Function (MRF) generated from waveform modeling to validate the ERF algorithm.

Selection of strong-motion stations

1. Slip distribution, along with the seismic intensity distribution maps (JMA, 1996; ShakeMap, 2017), used to select stations within the inferred azimuthal range and seismic intensity > 3.

OPEN

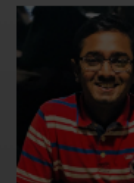
6. Summary

1. HHT-based **ERF captures the earthquake source energy release**, with a **higher resolution** offered by HHT as compared to Fourier analysis methods and wavelet transform.
2. **ERF retains frequency information**, is computationally faster for a rapid interpretation of an event, and **does not entail assumptions** of the fault geometry and velocity structure. These are clear advantages over the traditional MRF.
3. **ERF captures complex ruptures** (2005 Miyagi-Oki event) and sub-events or

2. Motivation

2. Interplate earthquakes, originating on the plate interface, show enhanced high-frequency energy (HFE) with increasing depth (Lay et al., 2012).
3. Outer-rise intraplate earthquakes produce enhanced HFE and ground shaking despite their high epicentral distances (Ye et al., 2013).
4. Intraslab earthquakes originate within the subduction slab (usually beneath population centers). They are more damaging than other similar Mw events due to enhanced HFE release and associated ground motion in a short duration, along with higher stress drop, increasing with depth (Choy et al., 2001; Okal and Kirby, 2002).
5. Conventional time-frequency analysis methods (Fourier transform, short-time Fourier transform, continuous wavelet transform) are deficient in resolving the above properties. They have a priori defined bases, are not suitable for nonlinear and nonstationary earthquake signals, and have limited resolution (Huang et al., 1998; Tary et al., 2014).
6. **Hilbert-Huang Transform (HHT)** overcomes these drawbacks and provides instantaneous frequency and energy, which we leverage to analyze energy release from five earthquakes, originating in different tectonic settings and depths.

n: A Hilbert-Huang



4. Methodology

Waveform inversion of teleseismic data

1. Kikuchi-Kanamori body-wave inversion program (Kikuchi and Kanamori, 1991) used for the analysis.
2. Moment Rate Function (MRF) generated from waveform modeling to validate the ERF algorithm.

Selection of strong-motion stations

1. Slip distribution, along with the seismic intensity distribution maps (JMA, 1996; ShakeMap, 2017), used to select stations within the inferred azimuthal range and seismic intensity > 3.

OPEN

6. Summary

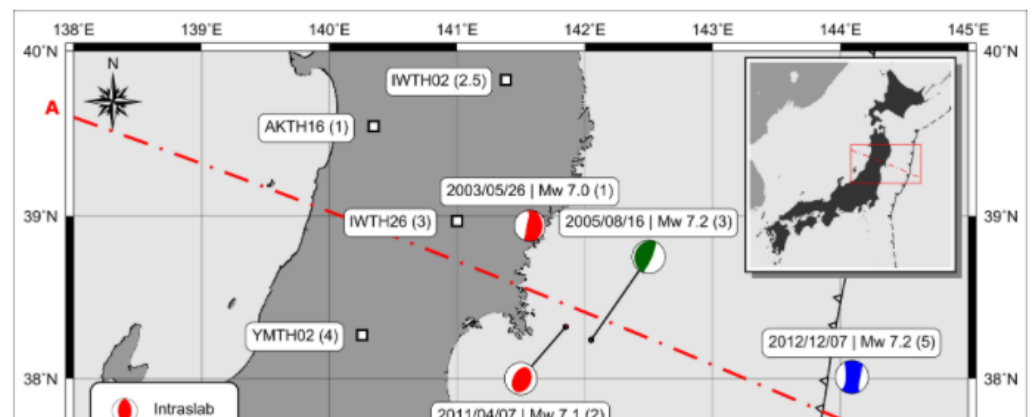
1. HHT-based **ERF captures the earthquake source energy release**, with a **higher resolution** offered by HHT as compared to Fourier analysis methods and wavelet transform.
2. **ERF retains frequency information**, is computationally faster for a rapid interpretation of an event, and **does not entail assumptions** of the fault geometry and velocity structure. These are clear advantages over the traditional MRF.
3. **ERF captures complex ruptures** (2005 Miyagi-Oki event) and sub-events or

3. Data

1. **Teleseismic data** from International Research Institutions for Seismology (IRIS). P and SH waveforms from 30-40 stations, epicentral distance 30° to 90°.
2. **Strong-motion acceleration data** from KiK-net, National Research Institute for Earth Science and Disaster Resilience (NIED, Japan). Data from the **vertical component of borehole sensors** (> 100 m depth) used in the analysis.

Event Number	Event Date (YYYY-MM-DD)	Event Time (hh:mm:ss.s)	Longitude (°E)	Latitude (°N)	Depth (km)	M _w	Tectonic Setting
1	2003-05-26	09:24:38.8	141.57	38.94	61.0	7.0	Intraslab
2	2011-04-07	14:32:50.6	141.85	38.32	53.3	7.1	
3	2005-08-16	02:46:40.3	142.05	38.24	37.0	7.2	Interplate
4	2008-07-19	02:39:34.8	142.42	37.47	21.8	6.9	
5	2012-12-07	08:18:34.9	144.09	38.01	57.8	7.2	Intraplate
		08:18:46.9	143.83	37.77	19.5	7.2	

Table: Earthquake details (from GCMT).



4. Methodology

Waveform inversion of teleseismic data

1. Kikuchi-Kanamori body-wave inversion program (Kikuchi and Kanamori, 1991) used for the analysis.
2. Moment Rate Function (MRF) generated from waveform modeling to validate the ERF algorithm.

Selection of strong-motion stations

1. Slip distribution, along with the seismic intensity distribution maps (JMA, 1996; ShakeMap, 2017), used to select stations within the inferred azimuthal range and seismic intensity > 3.

6. Summary

1. HHT-based ERF captures the earthquake source energy release, with a **higher resolution** offered by HHT as compared to Fourier analysis methods and wavelet transform.
2. ERF retains frequency information, is computationally faster for a rapid interpretation of an event, and **does not entail assumptions** of the fault geometry and velocity structure. These are clear advantages over the traditional MRF.
3. ERF captures complex ruptures (2005 Miyagi-Oki event) and sub-events or

3. Data

Event Number	Event Date (YYYY-MM-DD)	Event Time (hh:mm:ss.s)	Longitude (°E)	Latitude (°N)	Depth (km)	M _w	Tectonic Setting
1	2003-05-26	09:24:38.8	141.57	38.94	61.0	7.0	Intraslab
2	2011-04-07	14:32:50.6	141.85	38.32	53.3	7.1	
3	2005-08-16	02:46:40.3	142.05	38.24	37.0	7.2	Interplate
4	2008-07-19	02:39:34.8	142.42	37.47	21.8	6.9	
5	2012-12-07	08:18:34.9	144.09	38.01	57.8	7.2	Intraplate
		08:18:46.9	143.83	37.77	19.5	7.2	

Table: Earthquake details (from GCMT).

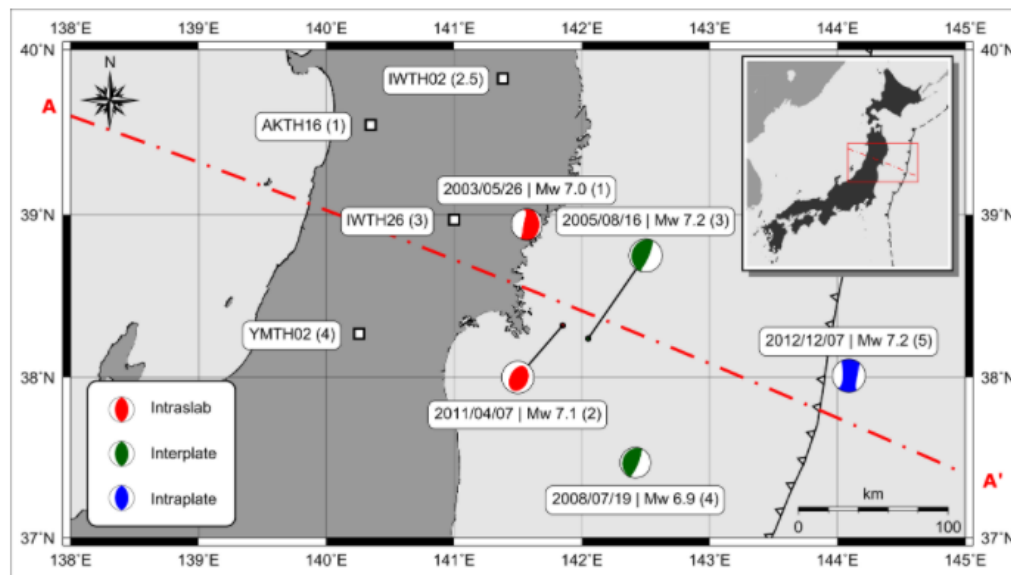
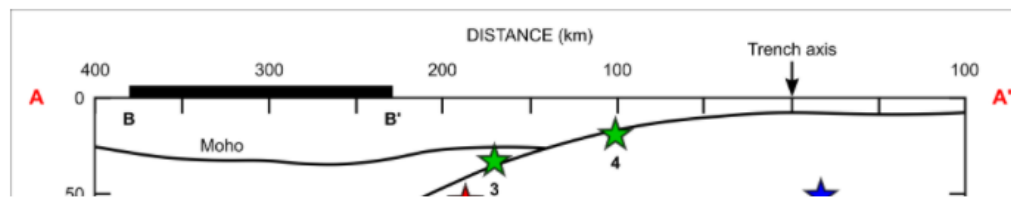


Figure: Map of the study region showing the five earthquakes and corresponding stations used for analysis.



4. Methodology

Waveform inversion of teleseismic data

1. Kikuchi-Kanamori body-wave inversion program (Kikuchi and Kanamori, 1991) used for the analysis.
2. Moment Rate Function (MRF) generated from waveform modeling to validate the ERF algorithm.

Selection of strong-motion stations

1. Slip distribution, along with the seismic intensity distribution maps (JMA, 1996; ShakeMap, 2017), used to select stations within the inferred azimuthal range and seismic intensity > 3.

6. Summary

1. HHT-based ERF captures the earthquake source energy release, with a higher resolution offered by HHT as compared to Fourier analysis methods and wavelet transform.
2. ERF retains frequency information, is computationally faster for a rapid interpretation of an event, and does not entail assumptions of the fault geometry and velocity structure. These are clear advantages over the traditional MRF.
3. ERF captures complex ruptures (2005 Miyagi-Oki event) and sub-events or

3. Data

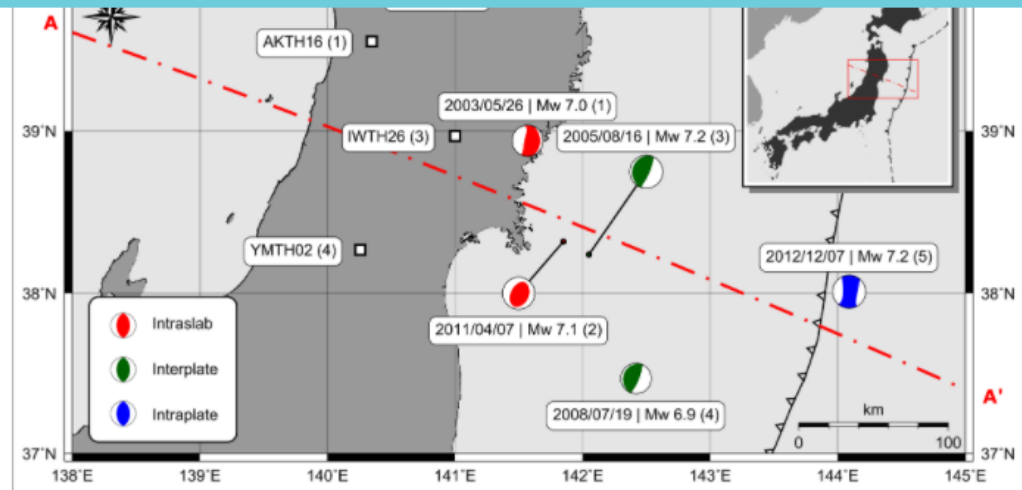


Figure: Map of the study region showing the five earthquakes and corresponding stations used for analysis.

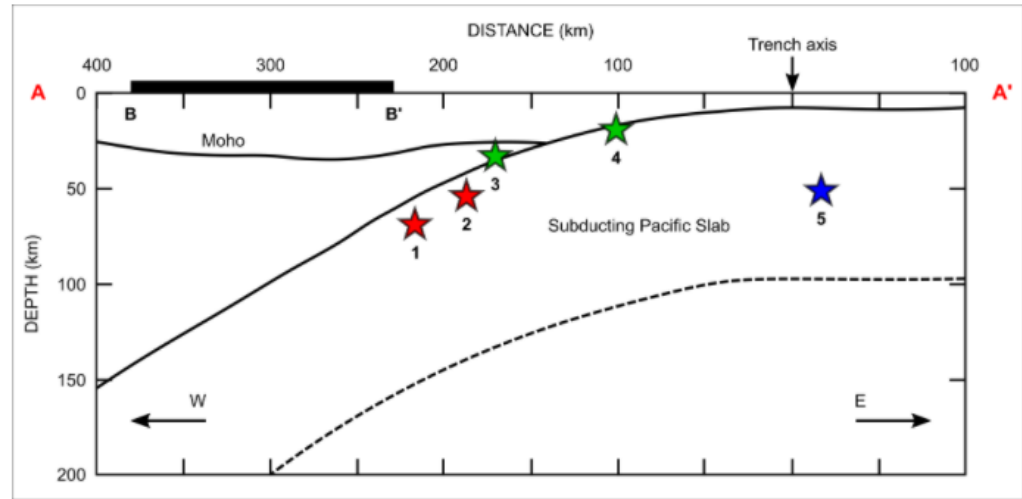


Figure: Cross-section showing the event distance from the trench, and depth, in km.

4. Methodology

- Waveform inversion of teleseismic data**
1. Kikuchi-Kanamori body-wave inversion program (Kikuchi and Kanamori, 1991) used for the analysis.
 2. Moment Rate Function (MRF) generated from waveform modeling to validate the ERF algorithm.
- Selection of strong-motion stations**
1. Slip distribution, along with the seismic intensity distribution maps (JMA, 1996; ShakeMap, 2017), used to select stations within the inferred azimuthal range and seismic intensity > 3.

6. Summary

1. HHT-based ERF captures the earthquake source energy release, with a higher resolution offered by HHT as compared to Fourier analysis methods and wavelet transform.
2. ERF retains frequency information, is computationally faster for a rapid interpretation of an event, and does not entail assumptions of the fault geometry and velocity structure. These are clear advantages over the traditional MRF.
3. ERF captures complex ruptures (2005 Miyagi-Oki event) and sub-events or



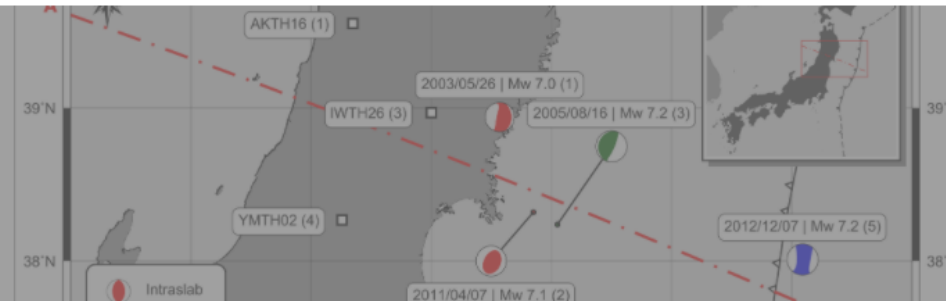
3. Data



1. **Teleseismic data** from International Research Institutions for Seismology (IRIS). P and SH waveforms from 30-40 stations, epicentral distance 30° to 90°.

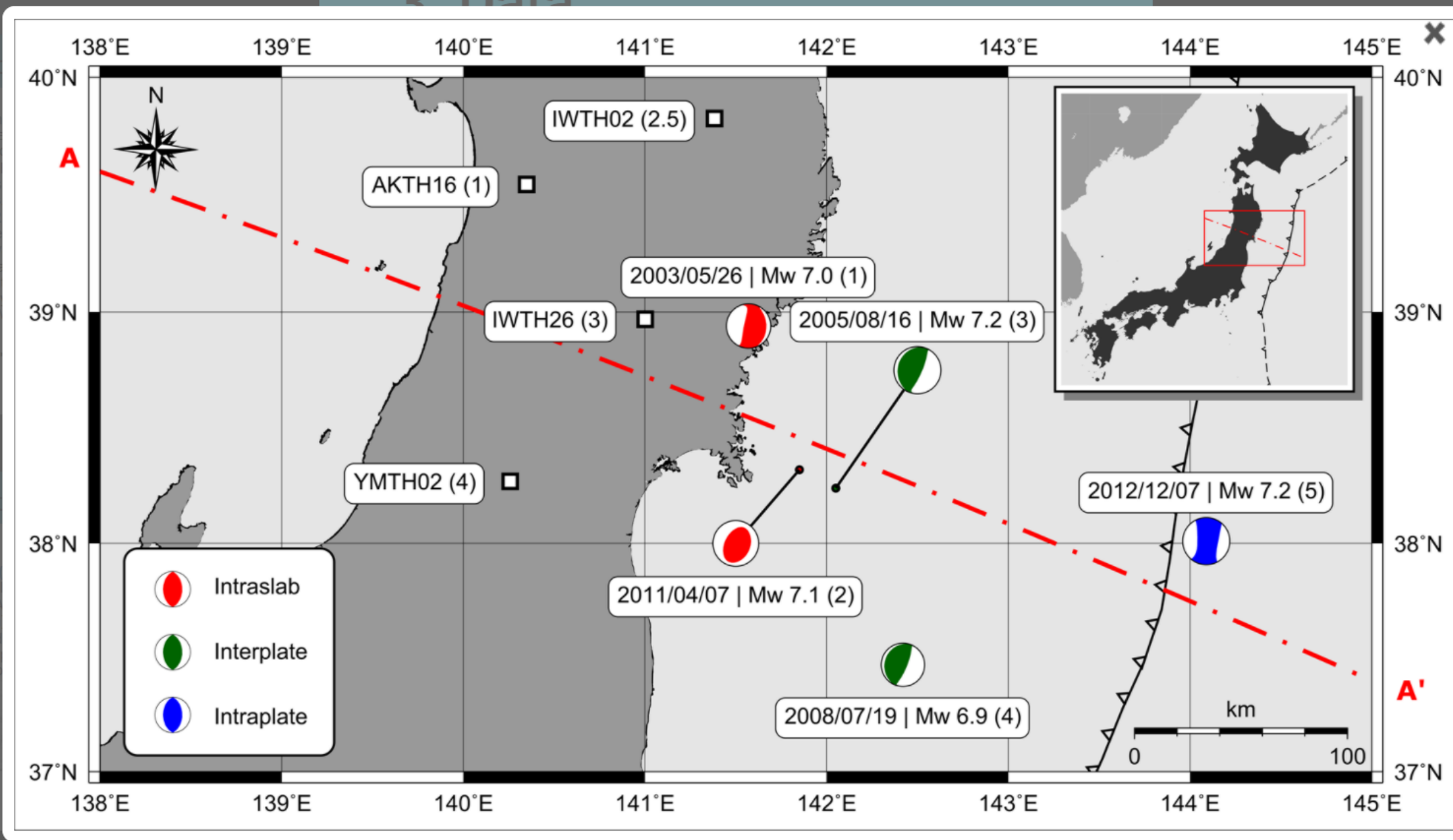
Event Number	Event Date (YYYY-MM-DD)	Event Time (hh:mm:ss.s)	Longitude (°E)	Latitude (°N)	Depth (km)	M _w	Tectonic Setting
1	2003-05-26	09:24:38.8	141.57	38.94	61.0	7.0	Intraslab
2	2011-04-07	14:32:50.6	141.85	38.32	53.3	7.1	
3	2005-08-16	02:46:40.3	142.05	38.24	37.0	7.2	Interplate
4	2008-07-19	02:39:34.8	142.42	37.47	21.8	6.9	
5	2012-12-07	08:18:34.9 08:18:46.9	144.09 143.83	38.01 37.77	57.8 19.5	7.2 7.2	Intraplate

1. 26 May 2003 Miyagi Intraslab Earthquake (Mw 7.0, depth 67.0 km)
 - Up-dip slip (towards east-northeast).
 - Station AKTH16, WNW (305.98° azimuth), seismic intensity (SI) 4.
 - Single, dominant, ~10 s energy pulse captured by both the ERF and MRF, along with a weaker tail.



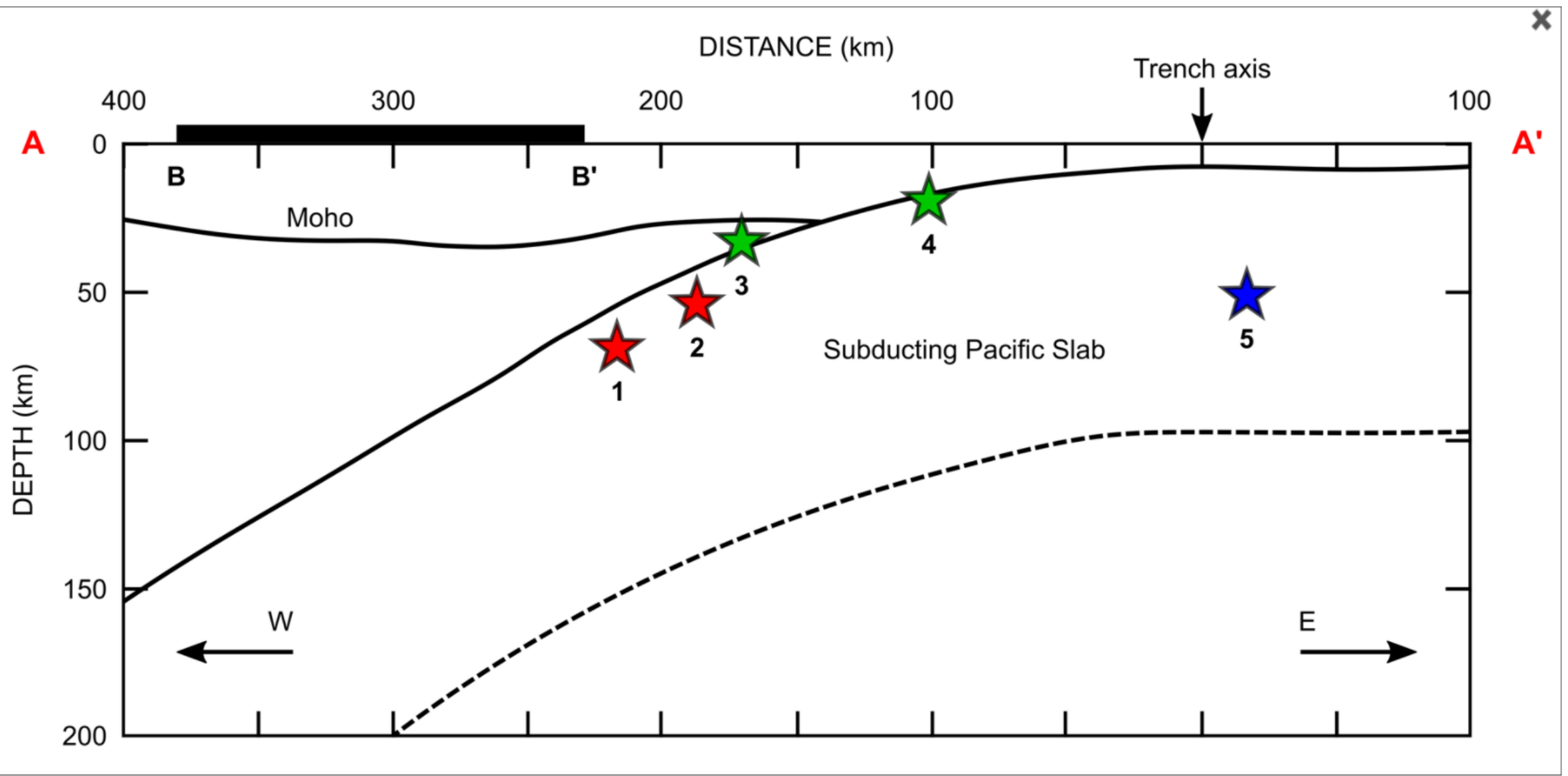
1. HHT-based ERF captures the earthquake source energy release with a higher resolution offered by HHT as compared to Fourier analysis methods and wavelet transform.
2. ERF retains frequency information, is computationally faster for a rapid interpretation of an event, and does not entail assumptions of the fault geometry and velocity structure. These are clear advantages over the traditional MRF.
3. ERF captures complex ruptures (2005 Miyagi-Oki event) and sub-events or

3. Data



[km] 1 2 Subducting Pacific Slab

3 Data



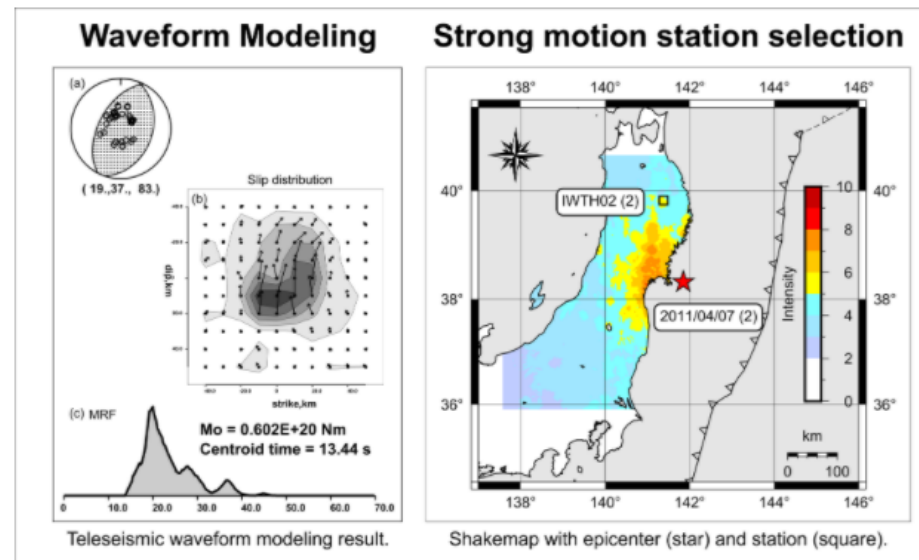
4. Methodology

Waveform inversion of teleseismic data

1. Kikuchi-Kanamori body-wave inversion program (Kikuchi and Kanamori, 1991) used for the analysis.
2. Moment Rate Function (MRF) generated from waveform modeling to validate the ERF algorithm.

Selection of strong-motion stations

1. Slip distribution, along with the seismic intensity distribution maps (JMA, 1996; ShakeMap, 2017), used to select stations within the inferred azimuthal range and seismic intensity > 3.



Key Points

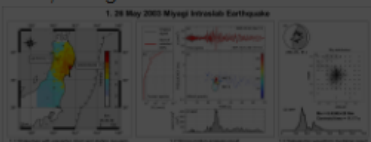
Specific Intrinsic Mode Functions (IMFs) represent energy release at the earthquake source.
Energy Rate Functions (ERFs) generated from Hilbert spectral analysis of such IMF combinations.
Proposed ERFs match well with the Moment Rate Functions (MRFs) from teleseismic waveform modeling.
ERF-MRF match is controlled by the station azimuth and shaking intensity, and frequency and energy-based selection of IMFs.

OPEN

Results

16 May 2003 Miyagi Intralab Earthquake (Mw 7.0, depth 67.0 km)

- Up-dip slip (towards east-northeast).
- Station AKTH16, WNW (305.98° azimuth), seismic intensity (SI) 4.
- Single, dominant, ~10 s energy pulse captured by both the ERF and MRF, along with a weaker tail.



OPEN

4. Methodology

Waveform inversion of teleseismic data

1. Kikuchi-Kanamori body-wave inversion program (Kikuchi and Kanamori, 1991) used for the analysis.
2. Moment Rate Function (MRF) generated from waveform modeling to validate the ERF algorithm.

Selection of strong-motion stations

1. Slip distribution, along with the seismic intensity distribution maps (JMA, 1996; ShakeMap, 2017), used to select stations within the inferred azimuthal range and seismic intensity > 3.

OPEN

6. Summary

1. HHT-based ERF captures the earthquake source energy release, with a higher resolution offered by HHT as compared to Fourier analysis methods and wavelet transform.
2. ERF retains frequency information, is computationally faster for a rapid interpretation of an event, and does not entail assumptions of the fault geometry and velocity structure. These are clear advantages over the traditional MRF.
3. ERF captures complex ruptures (2005 Miyagi-Oki event) and sub-events or

OPEN

4. Methodology

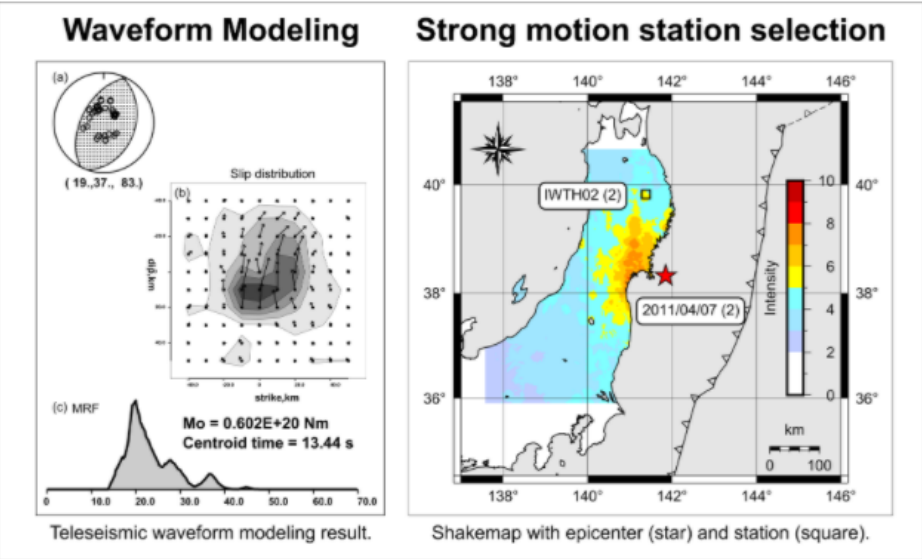


Figure: Waveform modeling results. Shakemap (along with slip distribution), used for strong-motion station-selection.

HHT-based strong-motion analysis

1. Hilbert-Huang Transform (HHT) is a combination of Empirical Mode Decomposition (EMD) and Hilbert Spectral Analysis (HSA) (Huang et al., 1998).
2. EMD decomposes the data into multiple frequency components (IMFs).
3. IMFs selected in the frequency range 0.1 to 3 Hz. Hilbert energy spectrum, a time-frequency-energy

4. Methodology

Waveform inversion of teleseismic data

1. Kikuchi-Kanamori body-wave inversion program (Kikuchi and Kanamori, 1991) used for the analysis.
2. Moment Rate Function (MRF) generated from waveform modeling to validate the ERF algorithm.

Selection of strong-motion stations

1. Slip distribution, along with the seismic intensity distribution maps (JMA, 1996; ShakeMap, 2017), used to select stations within the inferred azimuthal range and seismic intensity > 3.

6. Summary

1. HHT-based ERF captures the earthquake source energy release, with a higher resolution offered by HHT as compared to Fourier analysis methods and wavelet transform.
2. ERF retains frequency information, is computationally faster for a rapid interpretation of an event, and does not entail assumptions of the fault geometry and velocity structure. These are clear advantages over the traditional MRF.
3. ERF captures complex ruptures (2005 Miyagi-Oki event) and sub-events or

Key Points

Specific Intrinsic Mode Functions (IMFs) represent energy release at the earthquake source.
Energy Rate Functions (ERFs) generated from Hilbert spectral analysis of such IMF combinations.
Proposed ERFs match well with the Moment Rate Functions (MRFs) from teleseismic waveform modeling.
ERF-MRF match is controlled by the station azimuth and shaking intensity, and frequency and energy-based selection of IMFs.

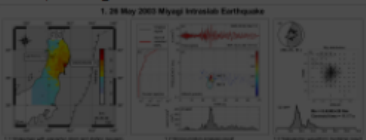
Short video explaining our work:

OPEN

Results

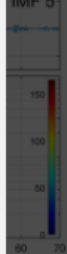
16 May 2003 Miyagi Intralab Earthquake (Mw 7.0, depth 67.0 km)

- Up-dip slip (towards east-northeast).
- Station AKTH16, WNW (305.98° azimuth), seismic intensity (SI) 4.
- Single, dominant, ~10 s energy pulse captured by both the ERF and MRF, along with a weaker tail.



OPEN

IMF 5



ACT

REFERENCES

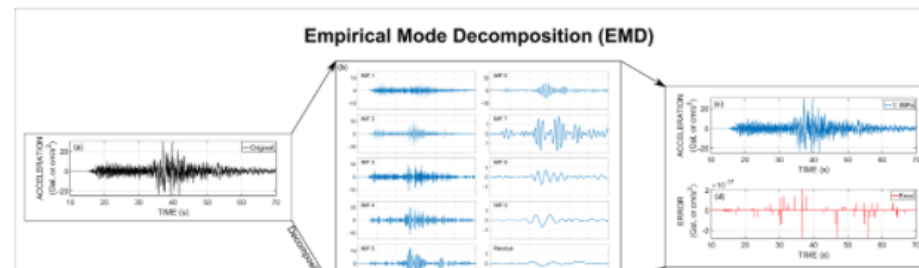
CONTACT AUTHOR

GET IP

4. Methodology

HHT-based strong-motion analysis

1. Hilbert-Huang Transform (HHT) is a combination of Empirical Mode Decomposition (**EMD**) and Hilbert Spectral Analysis (**HSA**) (Huang et al., 1998).
2. EMD decomposes the data into multiple frequency components (IMFs).
3. **IMFs** selected in the **frequency range 0.1 to 3 Hz**. Hilbert energy spectrum, a time-frequency-energy representation of the signal, generated for each selected IMF.
4. **Maximum amplitude-squared values** obtained from the Hilbert spectra of selected IMFs used to generate the Energy Rate Function (ERF).
5. ERF is representative of energy release at the earthquake source, validated by its comparison with the MRF.



4. Methodology

Waveform inversion of teleseismic data

1. Kikuchi-Kanamori body-wave inversion program (Kikuchi and Kanamori, 1991) used for the analysis.
2. Moment Rate Function (MRF) generated from waveform modeling to validate the ERF algorithm.

Selection of strong-motion stations

1. Slip distribution, along with the seismic intensity distribution maps (JMA, 1996; ShakeMap, 2017), used to select stations within the inferred azimuthal range and seismic intensity > 3.

6. Summary

1. HHT-based **ERF captures the earthquake source energy release**, with a **higher resolution** offered by HHT as compared to Fourier analysis methods and wavelet transform.
2. **ERF retains frequency information**, is computationally faster for a rapid interpretation of an event, and **does not entail assumptions** of the fault geometry and velocity structure. These are clear advantages over the traditional MRF.
3. **ERF captures complex ruptures** (2005 Miyagi-Oki event) and sub-events or

4. Methodology

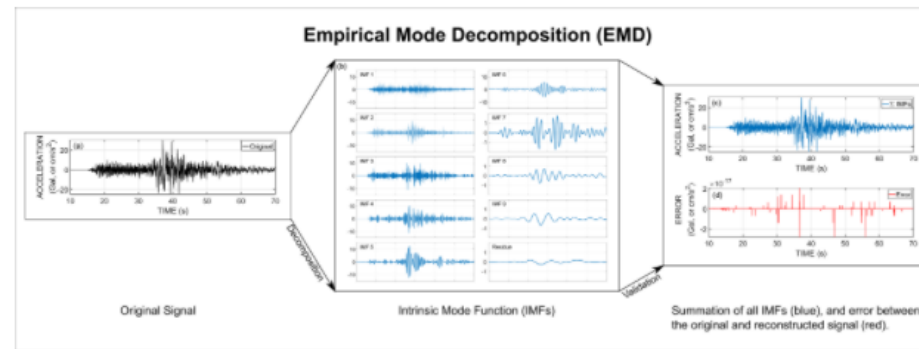


Figure: EMD and validation.

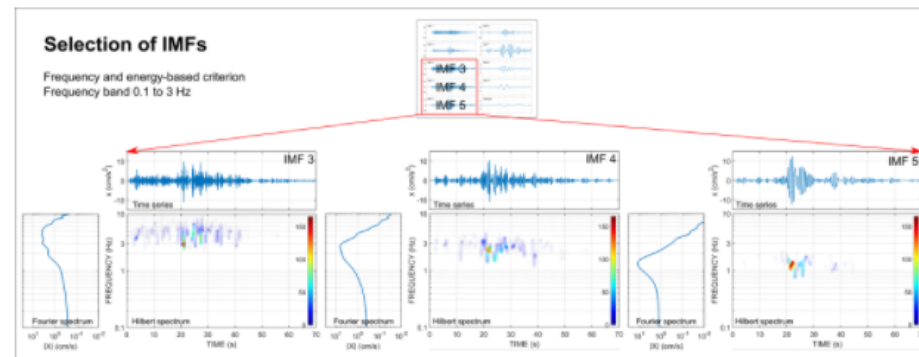
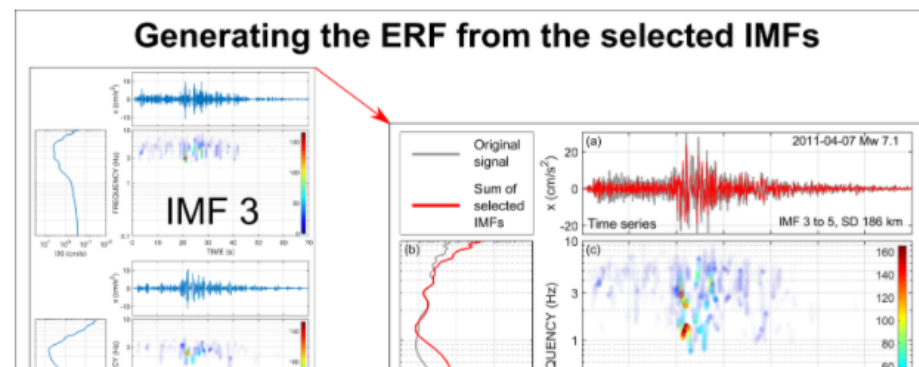


Figure: Selection of IMFs.



Key Points

Specific Intrinsic Mode Functions (IMFs) represent energy release at the earthquake source.

Energy Rate Functions (ERFs) generated from Hilbert spectral analysis of such IMF combinations.

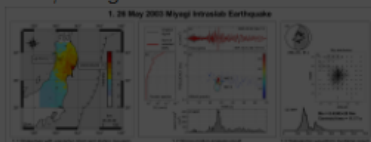
Proposed ERFs match well with the Moment Rate Functions (MRFs) from teleseismic waveform modeling.

ERF-MRF match is controlled by the station azimuth and shaking intensity, and frequency and energy-based selection of IMFs.

Results

26 May 2003 Miyagi Intralab Earthquake (Mw 7.0, depth 67.0 km)

- Up-dip slip (towards east-northeast).
- Station AKTH16, WNW (305.98° azimuth), seismic intensity (SI) 4.
- Single, dominant, ~10 s energy pulse captured by both the ERF and MRF, along with a weaker tail.



4. Methodology

Waveform inversion of teleseismic data

1. Kikuchi-Kanamori body-wave inversion program (Kikuchi and Kanamori, 1991) used for the analysis.
2. Moment Rate Function (MRF) generated from waveform modeling to validate the ERF algorithm.

Selection of strong-motion stations

1. Slip distribution, along with the seismic intensity distribution maps (JMA, 1996; ShakeMap, 2017), used to select stations within the inferred azimuthal range and seismic intensity > 3.

6. Summary

1. HHT-based ERF captures the earthquake source energy release, with a **higher resolution** offered by HHT as compared to Fourier analysis methods and wavelet transform.
2. ERF retains frequency information, is computationally faster for a rapid interpretation of an event, and **does not entail assumptions** of the fault geometry and velocity structure. These are clear advantages over the traditional MRF.
3. ERF captures complex ruptures (2005 Miyagi-Oki event) and sub-events or

4. Methodology

Generating the ERF from the selected IMFs

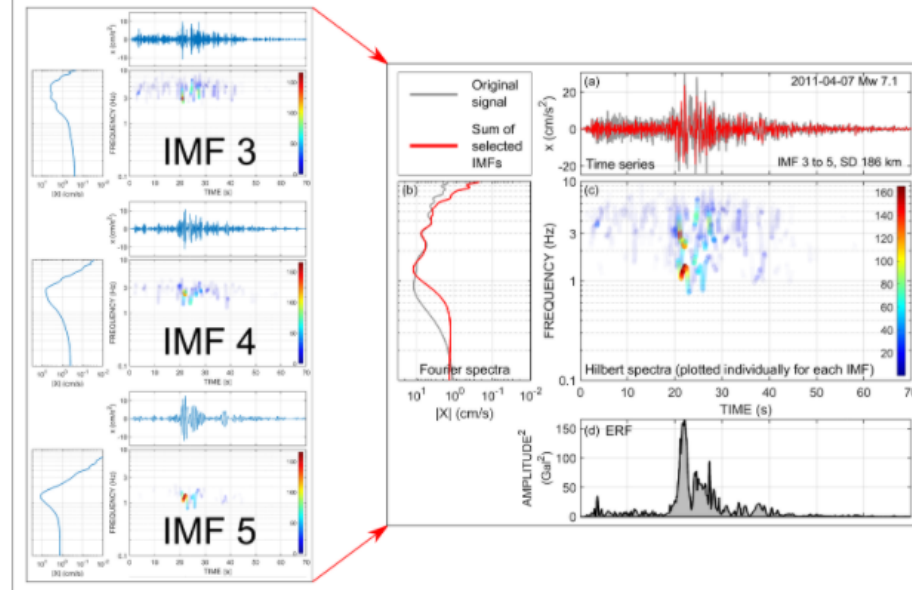
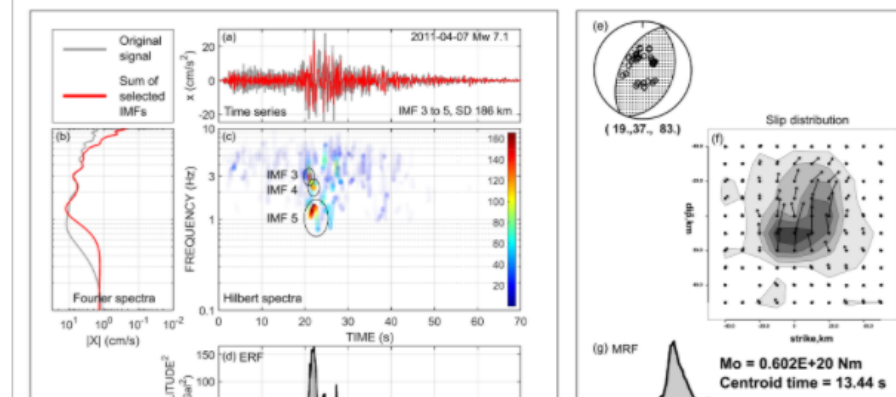


Figure: Using the selected IMFs to generate the Energy Rate Function (ERF).

Comparing the ERF and MRF



4. Methodology

Waveform inversion of teleseismic data

1. Kikuchi-Kanamori body-wave inversion program (Kikuchi and Kanamori, 1991) used for the analysis.
2. Moment Rate Function (MRF) generated from waveform modeling to validate the ERF algorithm.

Selection of strong-motion stations

1. Slip distribution, along with the seismic intensity distribution maps (JMA, 1996; ShakeMap, 2017), used to select stations within the inferred azimuthal range and seismic intensity > 3.

6. Summary

1. HHT-based ERF captures the earthquake source energy release, with a higher resolution offered by HHT as compared to Fourier analysis methods and wavelet transform.
2. ERF retains frequency information, is computationally faster for a rapid interpretation of an event, and does not entail assumptions of the fault geometry and velocity structure. These are clear advantages over the traditional MRF.
3. ERF captures complex ruptures (2005 Miyagi-Oki event) and sub-events or

Comparing the ERF and MRF

Strong motion analysis result.

(a) Time series of acceleration x (cm/s²) vs Time (s) for 2011-04-07 Mw 7.1. IMFs 3 to 5, SD 186 km. Legend: Original signal (grey), Sum of selected IMFs (red).

(b) Fourier spectra of acceleration $|X|$ (cm/s) vs Frequency (Hz) on a log scale. Legend: Original signal (grey), Sum of selected IMFs (red).

(c) Hilbert spectra showing Frequency (Hz) vs Time (s) for IMF 3, IMF 4, and IMF 5. Color scale ranges from 20 to 160.

(d) ERF (Envelope of Residuals Function) Amplitude² (cm/s²) vs Time (s). Centroid time = 13.44 s.

Teleseismic waveform modeling result.

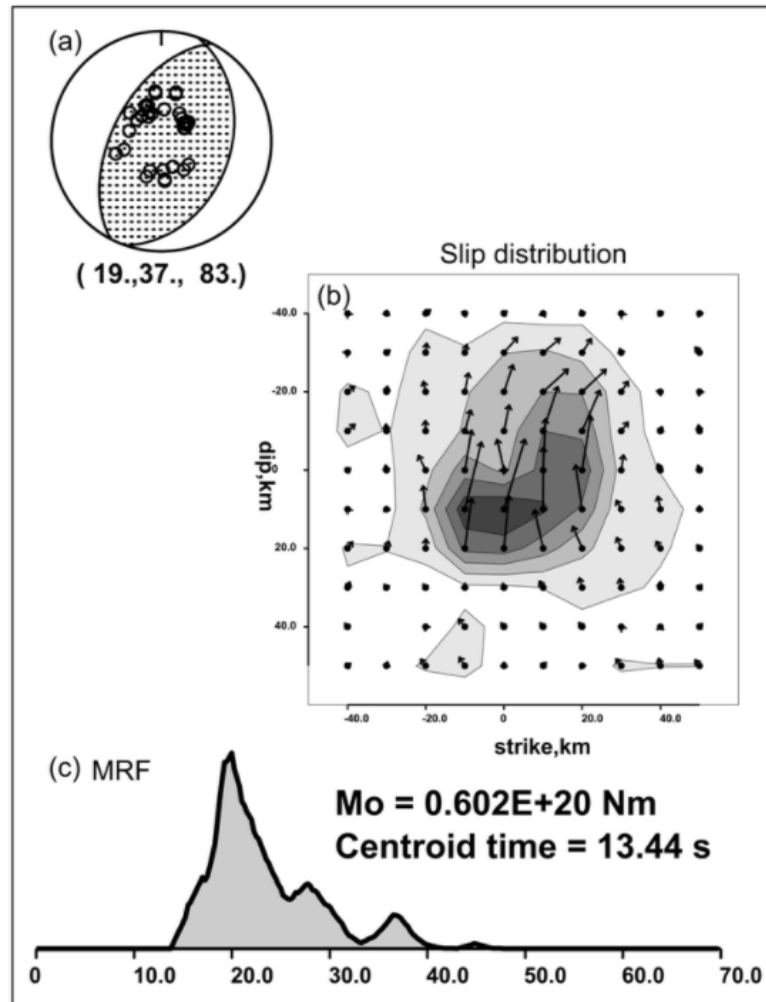
(e) Slip distribution map for the 2011-04-07 Mw 7.1 earthquake. Location: (19, 37, 83).

(f) Slip distribution map showing slip (cm) vs strike (km) and slip (cm) vs time (s).

(g) MRF (Model Residual Function) Amplitude² (cm/s²) vs Time (s). Centroid time = 13.44 s. $M_0 = 0.602E+20$ Nm.

1. **HHT-based ERF captures the earthquake source energy release**, with a **higher resolution** offered by HHT as compared to Fourier analysis methods and wavelet transform.
2. **ERF retains frequency information**, is computationally faster for a rapid interpretation of an event, and **does not entail assumptions** of the fault geometry and velocity structure. These are clear advantages over the traditional MRF.
3. **ERF captures complex ruptures** (2005 Miyagi-Oki event) and sub-events or

Waveform Modeling



Strong motion station selection

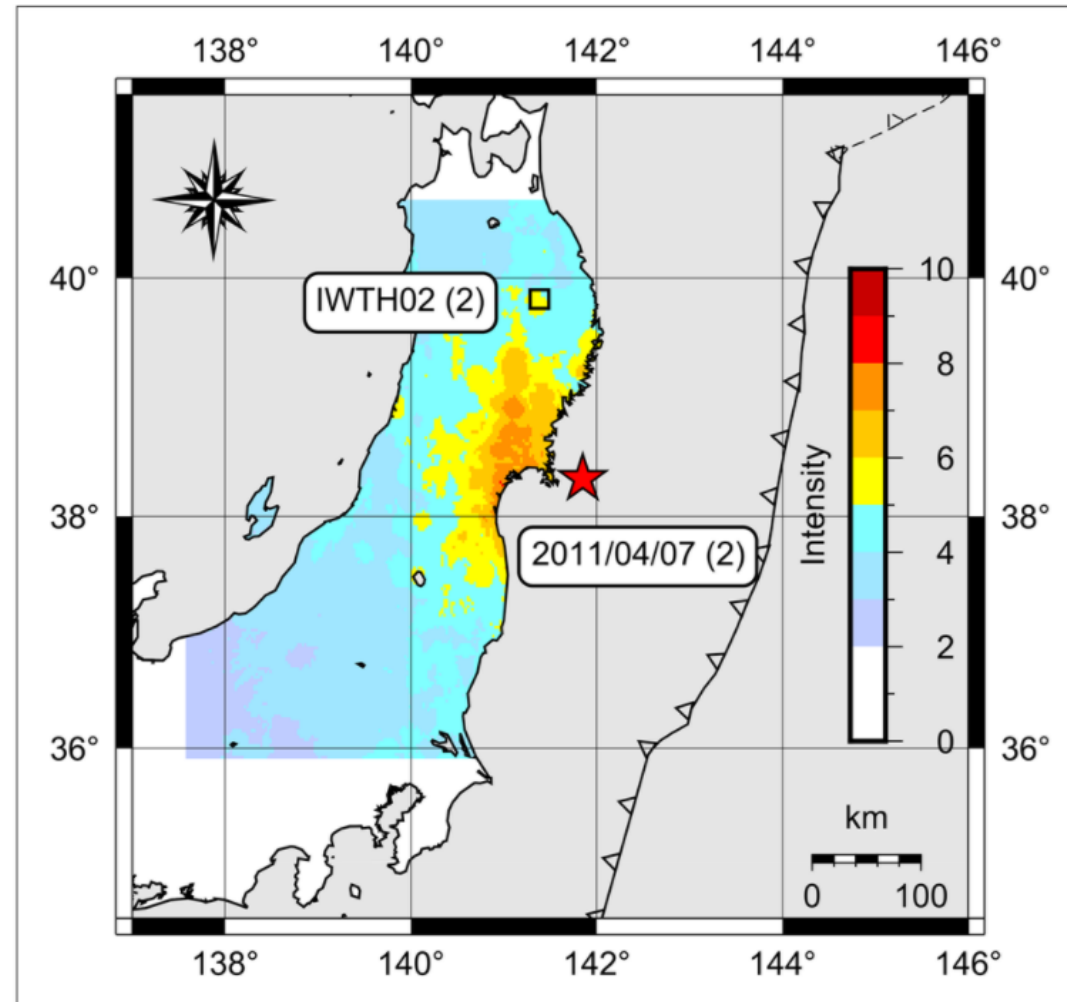


Figure: Waveform modeling results. Shakemap (along with

4. Methodology

Hilbert spectra of selected IMFs used to generate the Energy Rate Function (ERF)

Empirical Mode Decomposition (EMD)

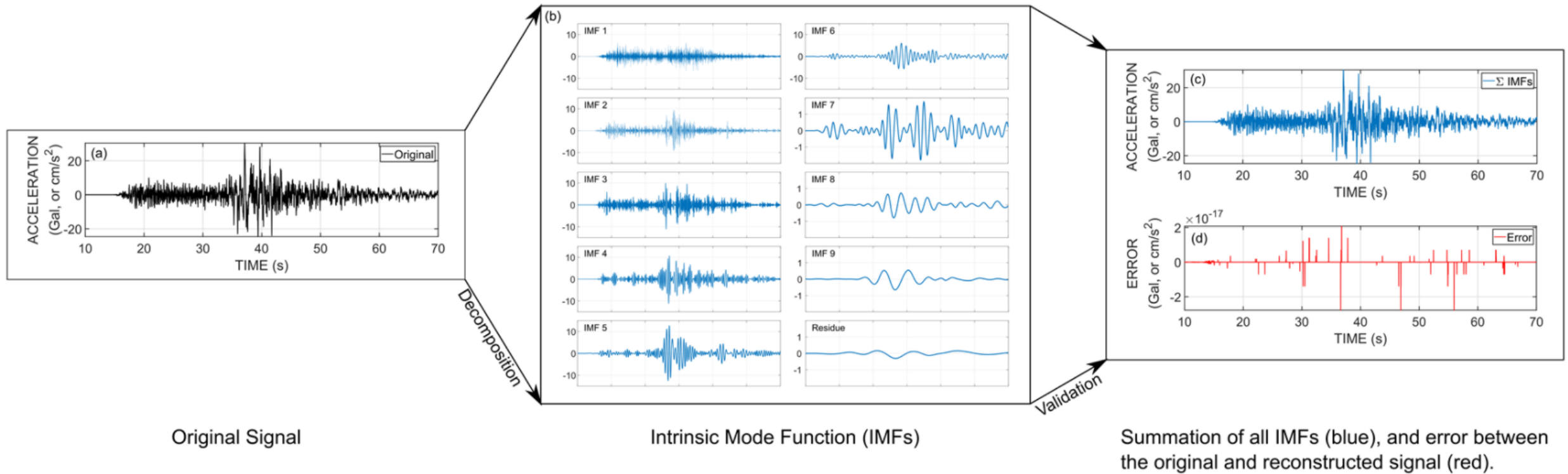


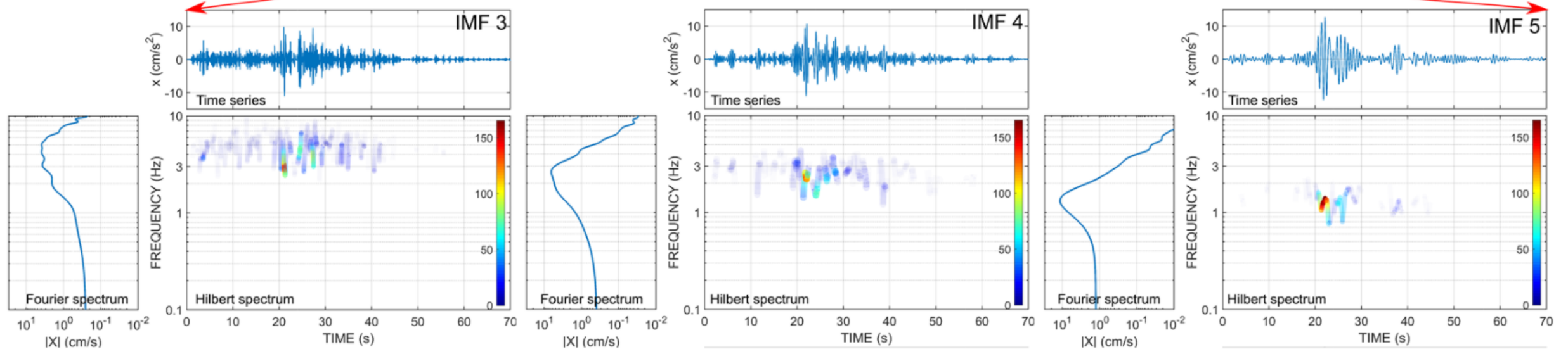
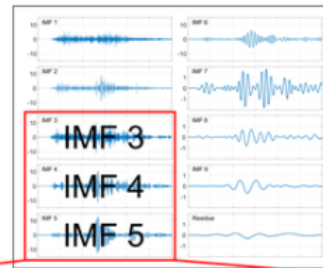
Figure: Selection of IMFs.

Generating the ERF from the selected IMFs

4. Methodology

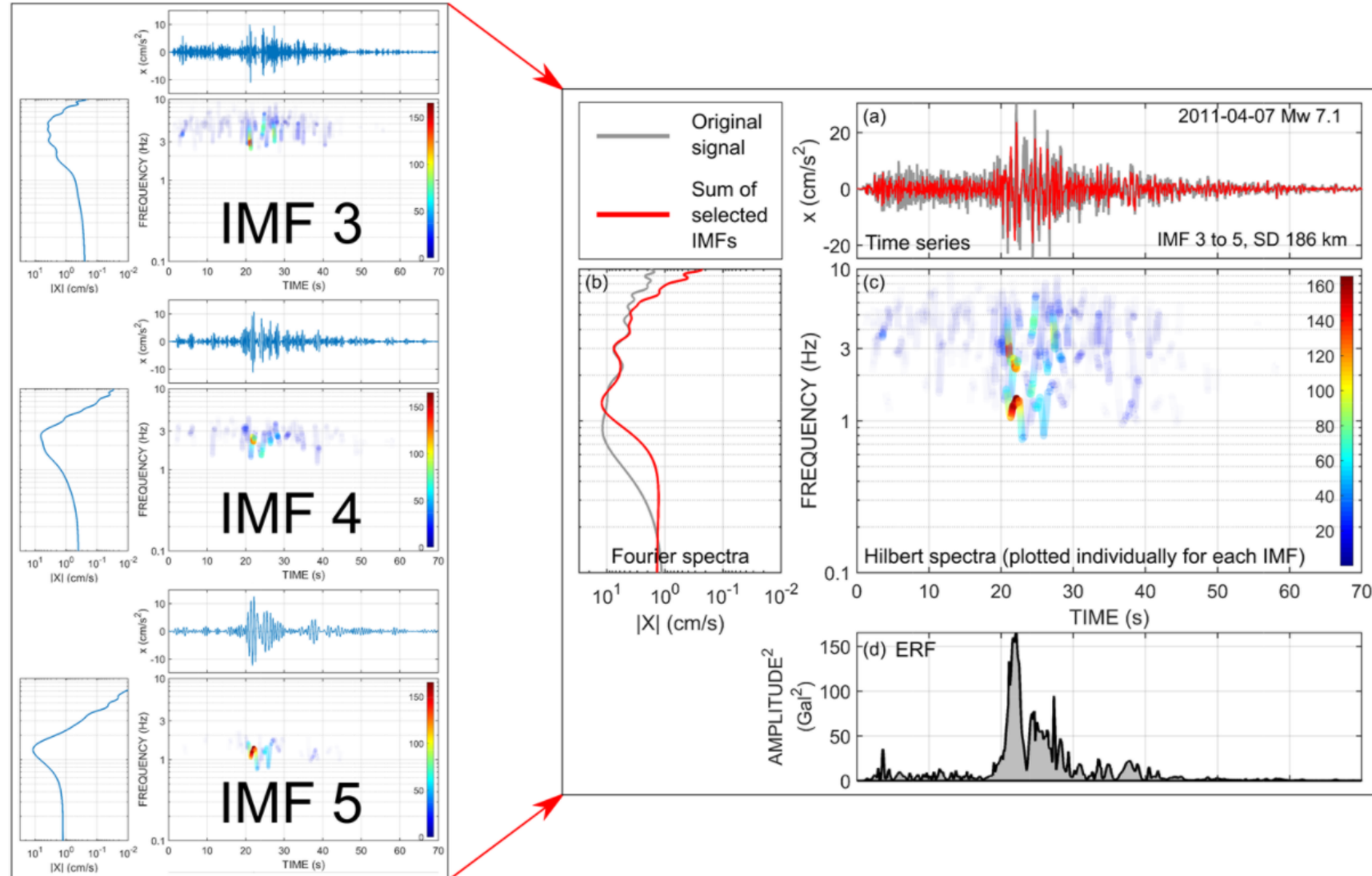
Selection of IMFs

Frequency and energy-based criterion
Frequency band 0.1 to 3 Hz



4 Methodology

Generating the ERF from the selected IMFs



1. Key Points

1. Specific Intrinsic Mode Functions (IMFs) represent energy release at the earthquake source.
2. Energy Rate Functions (ERFs) are derived from Hilbert spectral analysis and combinations.
3. Proposed ERFs match well with Moment Rate Functions (MRFs) for teleseismic waveform modeling.
4. ERF-MRF match is controlled by station azimuth and shaking intensity and frequency and energy-based selection of IMFs.

A short video explaining our work

OPEN

5. Results

1. 26 May 2003 Miyagi Intraslab Earthquake (Mw 7.0, depth 10 km)
 - Up-dip slip (towards east)
 - Station AKTH16, WNW (10° azimuth), seismic intensity 10
 - Single, dominant, ~10 s pulse captured by both the MRF, along with a weaker



OPEN

Methodology

The ERF (Energy Rate Function) (MRF) generated from the teleseismic waveform modeling to validate the ERF. The ERF, along with the seismic distribution maps (JMA, 1996; JMA, 2017), used to select stations preferred azimuthal range and intensity > 3.

Strong motion station selection

OPEN

Summary

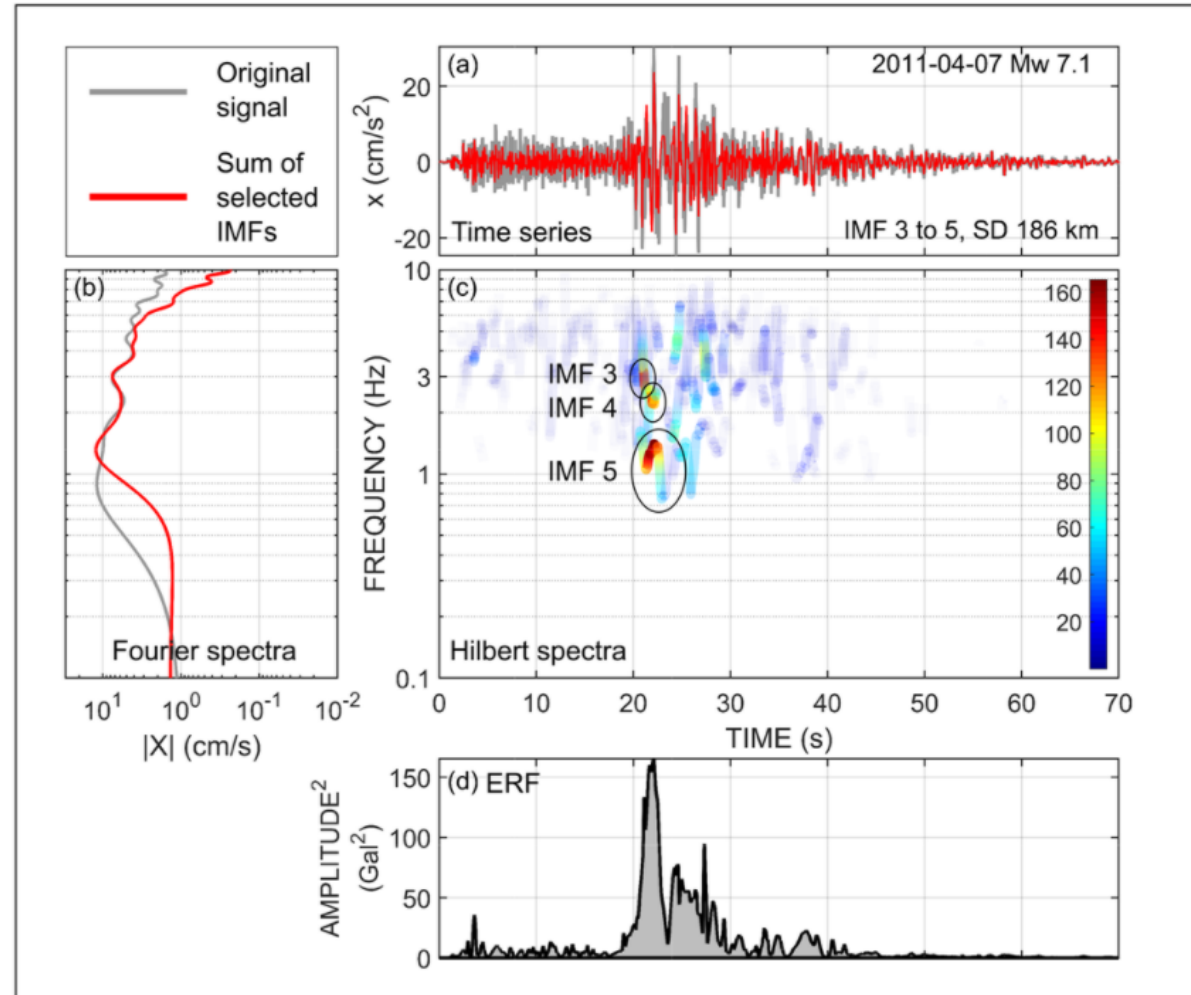
ERF captures the source energy release, offering higher resolution than Fourier analysis methods. ERF captures the frequency information, is useful for a rapid assessment of an event, and does not require assumptions of the fault geometry and velocity structure. These are advantages over the traditional methods.

ERF captures complex ruptures (2005 event) and sub-events or

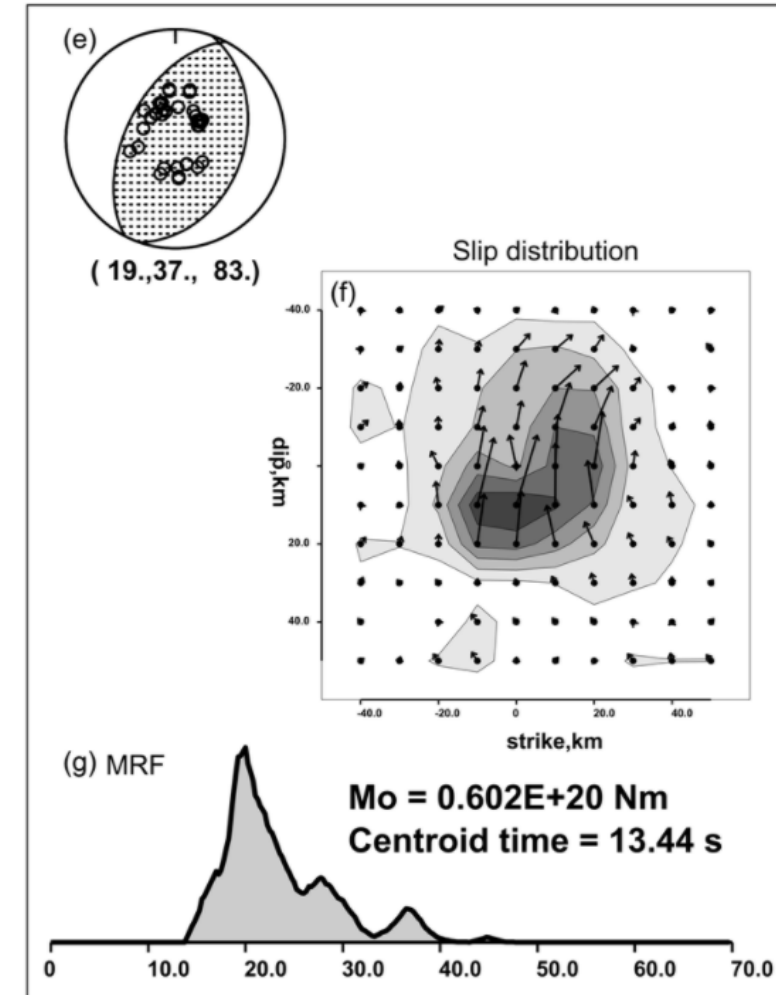
OPEN

4. Methodology

Comparing the ERF and MRF



Strong motion analysis result.

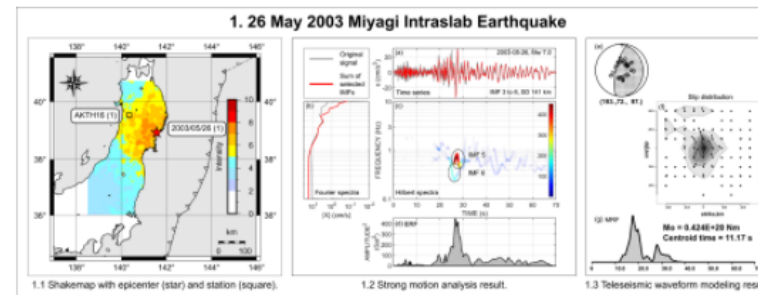


Teleseismic waveform modeling result.

5. Results

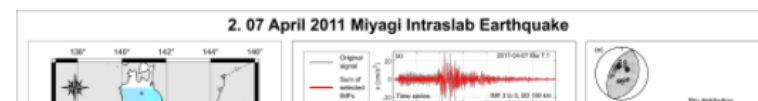
1. 26 May 2003 Miyagi Intralab Earthquake (Mw 7.0, depth 67.0 km)

- Up-dip slip (towards east-northeast).
- Station AKTH16, WNW (305.98° azimuth), seismic intensity (SI) 4.
- Single, dominant, ~10 s energy pulse captured by both the ERF and MRF, along with a weaker tail.



2. 07 April 2011 Miyagi Intralab Earthquake (Mw 7.1, depth 53.3 km)

- Slip direction northwest.
- Station IWTH02, north-northwest (345.73° azimuth), SI 6-lower.
- Single, dominant energy pulse with a peak at 20 seconds and decaying gradually up to 40 seconds captured by both the ERF and MRF.



1. Key Points

1. Specific Intrinsic Mode Functions (IMFs) represent energy release at the earthquake source.
2. Energy Rate Functions (ERFs) generated from Hilbert spectral analysis of such IMF combinations.
3. Proposed ERFs match well with the Moment Rate Functions (MRFs) from teleseismic waveform modeling.
4. ERF-MRF match is controlled by the station azimuth and shaking intensity, and frequency and energy-based selection of IMFs.

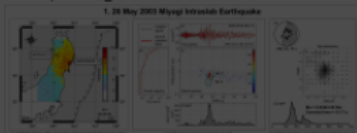
A short video explaining our work

OPEN

5. Results

1. 26 May 2003 Miyagi Intralab Earthquake (Mw 7.0, depth 67.0 km)

- Up-dip slip (towards east-northeast).
- Station AKTH16, WNW (305.98° azimuth), seismic intensity (SI) 4.
- Single, dominant, ~10 s energy pulse captured by both the ERF and MRF, along with a weaker tail.



OPEN

4. Methodology

2. Moment Rate Function (MRF) generated from waveform modeling to validate the ERF algorithm.

Selection of strong-motion stations

1. Slip distribution, along with the seismic intensity distribution maps (JMA, 1996; ShakeMap, 2017), used to select stations within the inferred azimuthal range and seismic intensity > 3.



OPEN

6. Summary

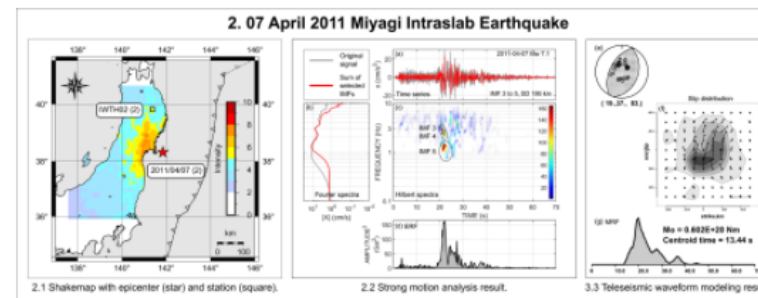
1. HHT-based ERF captures the earthquake source energy release, with a **higher resolution** offered by HHT as compared to Fourier analysis methods and wavelet transform.
2. ERF retains frequency information, is computationally faster for a rapid interpretation of an event, and **does not entail assumptions** of the fault geometry and velocity structure. These are clear advantages over the traditional MRF.
3. ERF captures complex ruptures (2005 Miyagi-Oki event) and sub-events or

OPEN

5. Results

2. 07 April 2011 Miyagi Intralab Earthquake (Mw 7.1, depth 53.3 km)

- Slip direction northwest.
- Station IWTH02, north-northwest (345.73° azimuth), SI 6-lower.
- Single, dominant energy pulse with a peak at 20 seconds and decaying gradually up to 40 seconds captured by both the ERF and MRF.



3. 16 August 2005 Miyagi-Oki Interplate Earthquake (Mw 7.2, depth 37.0 km)

- Station IWTH26, azimuth 309.76° , SI 5-upper.
- **Rough MRF** observed by [Lay et al. \(2012\)](#) and [Yaginuma et al. \(2006\)](#).
- ERF and MRF both match well with the above studies.
- A deeper interplate event, and shows **enrichment in high-frequency energy** (0.4 to 5 Hz range).

1. Key Points

1. Specific Intrinsic Mode Functions (IMFs) represent energy release at the earthquake source.
2. Energy Rate Functions (ERFs) generated from Hilbert spectral analysis of such IMF combinations.
3. Proposed ERFs match well with the Moment Rate Functions (MRFs) from teleseismic waveform modeling.
4. ERF-MRF match is controlled by the station azimuth and shaking intensity, and frequency and energy-based selection of IMFs.

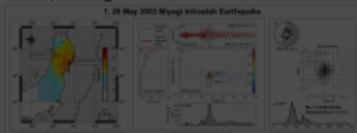
A short video explaining our work:

OPEN

5. Results

1. 26 May 2003 Miyagi Intralab Earthquake (Mw 7.0, depth 67.0 km)

- Up-dip slip (towards east-northeast).
- Station AKTH16, WNW (305.98° azimuth), seismic intensity (SI) 4.
- Single, dominant, ~ 10 s energy pulse captured by both the ERF and MRF, along with a weaker tail.



OPEN

4. Methodology

2. Moment Rate Function (MRF) generated from waveform modeling to validate the ERF algorithm.

Selection of strong-motion stations

1. Slip distribution, along with the seismic intensity distribution maps ([JMA, 1996](#); [ShakeMap, 2017](#)), used to select stations within the inferred azimuthal range and seismic intensity > 3 .



OPEN

6. Summary

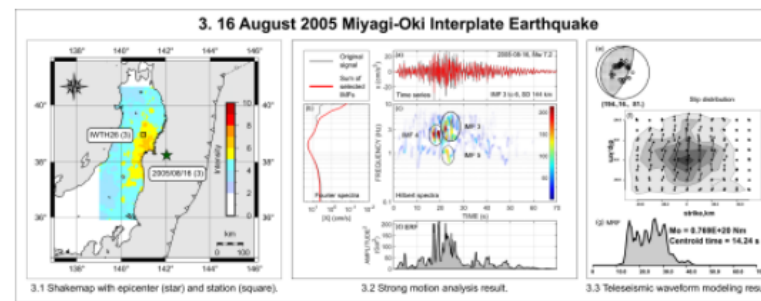
1. HHT-based ERF captures the earthquake source energy release, with a **higher resolution** offered by HHT as compared to Fourier analysis methods and wavelet transform.
2. ERF retains frequency information, is computationally faster for a rapid interpretation of an event, and **does not entail assumptions** of the fault geometry and velocity structure. These are clear advantages over the traditional MRF.
3. ERF captures complex ruptures (2005 Miyagi-Oki event) and sub-events or

OPEN

5. Results

3. 16 August 2005 Miyagi-Oki Interplate Earthquake (Mw 7.2, depth 37.0 km)

- Station IWTH26, azimuth 309.76°, SI 5-upper.
- **Rough MRF** observed by [Lay et al. \(2012\)](#) and [Yaginuma et al. \(2006\)](#).
- ERF and MRF both match well with the above studies.
- A deeper interplate event, and shows **enrichment in high-frequency energy** (0.4 to 5 Hz range).



4. 19 July 2008 Fukushima ken-Oki Interplate Earthquake (Mw 6.9, depth 21.8 km)

- Slip directed up-dip (east-southeast).
- Station YMTH02, north-northwest (azimuth 295.96°), SI 3.
- **ERF-MRF match** obtained even for **low SI** at the station location.
- A shallow interplate event; **low-frequency energy**

1. Key Points

1. Specific Intrinsic Mode Functions (IMFs) represent energy release at the earthquake source.
2. Energy Rate Functions (ERFs) generated from Hilbert spectral analysis of such IMF combinations.
3. Proposed ERFs match well with the Moment Rate Functions (MRFs) from teleseismic waveform modeling.
4. ERF-MRF match is controlled by the station azimuth and shaking intensity, and frequency and energy-based selection of IMFs.

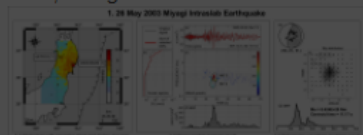
A short video explaining our work:

OPEN

5. Results

1. 26 May 2003 Miyagi Intraslab Earthquake (Mw 7.0, depth 67.0 km)

- Up-dip slip (towards east-northeast).
- Station AKTH16, WNW (305.98° azimuth), seismic intensity (SI) 4.
- Single, dominant, ~10 s energy pulse captured by both the ERF and MRF, along with a weaker tail.



OPEN

4. Methodology

2. Moment Rate Function (MRF) generated from waveform modeling to validate the ERF algorithm.

Selection of strong-motion stations

1. Slip distribution, along with the seismic intensity distribution maps ([JMA, 1996](#); [ShakeMap, 2017](#)), used to select stations within the inferred azimuthal range and seismic intensity > 3.



OPEN

6. Summary

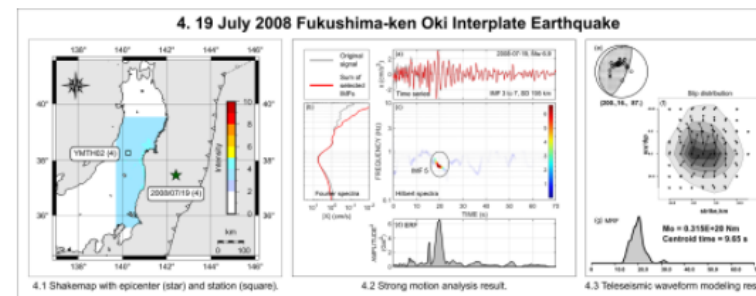
1. HHT-based ERF captures the **earthquake source energy release**, with a **higher resolution** offered by HHT as compared to Fourier analysis methods and wavelet transform.
2. **ERF retains frequency information**, is computationally faster for a rapid interpretation of an event, and **does not entail assumptions** of the fault geometry and velocity structure. These are clear advantages over the traditional MRF.
3. **ERF captures complex ruptures** (2005 Miyagi-Oki event) and sub-events or

OPEN

5. Results

4. 19 July 2008 Fukushima ken-Oki Interplate Earthquake (Mw 6.9, depth 21.8 km)

- Slip directed up-dip (east-southeast).
- Station YMTH02, north-northwest (azimuth 295.96°), SI 3.
- **ERF-MRF match** obtained even for **low SI** at the station location.
- A shallow interplate event; **low-frequency energy** (Ye et al., 2013).



5. 07 December 2012 Kamaishi Intraplate Earthquake (Mw 7.2, depth 50.8 km)

- Station IWTH02, azimuth 313.85°, SI 5-lower. Station approximately orthogonal to strike.
- Earthquake modeled as two independent events, deep thrust and shallow normal-faulting (Craig et al., 2014; Harada et al., 2013; Lay et al., 2013).
- **ERF and MRF** both show **two distinct pulses**,

1. Key Points

1. Specific Intrinsic Mode Functions (IMFs) represent energy release at the earthquake source.
2. Energy Rate Functions (ERFs) generated from Hilbert spectral analysis of such IMF combinations.
3. Proposed ERFs match well with the Moment Rate Functions (MRFs) from teleseismic waveform modeling.
4. ERF-MRF match is controlled by the station azimuth and shaking intensity, and frequency and energy-based selection of IMFs.

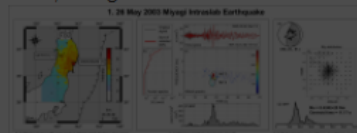
A short video explaining our work

OPEN

5. Results

1. 26 May 2003 Miyagi Intraslab Earthquake (Mw 7.0, depth 67.0 km)

- Up-dip slip (towards east-northeast).
- Station AKTH16, WNW (305.98° azimuth), seismic intensity (SI) 4.
- Single, dominant, ~10 s energy pulse captured by both the ERF and MRF, along with a weaker tail.



OPEN

4. Methodology

2. Moment Rate Function (MRF) generated from waveform modeling to validate the ERF algorithm.

Selection of strong-motion stations

1. Slip distribution, along with the seismic intensity distribution maps (JMA, 1996; ShakeMap, 2017), used to select stations within the inferred azimuthal range and seismic intensity > 3.



OPEN

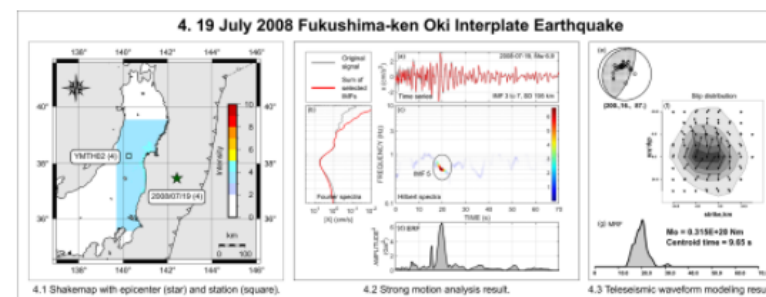
6. Summary

1. HHT-based ERF captures the earthquake source energy release, with a **higher resolution** offered by HHT as compared to Fourier analysis methods and wavelet transform.
2. ERF retains frequency information, is computationally faster for a rapid interpretation of an event, and **does not entail assumptions** of the fault geometry and velocity structure. These are clear advantages over the traditional MRF.
3. ERF captures complex ruptures (2005 Miyagi-Oki event) and sub-events or

OPEN

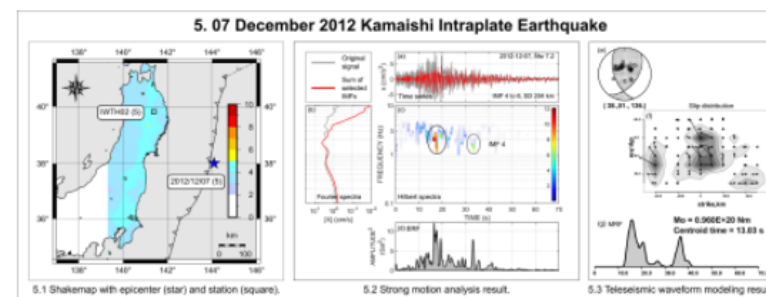
5. Results

(Ye et al., 2013).



5. 07 December 2012 Kamaishi Intraplate Earthquake (Mw 7.2, depth 50.8 km)

- Station IWTH02, azimuth 313.85°, SI 5-lower. Station approximately orthogonal to strike.
- Earthquake modeled as two independent events, deep thrust and shallow normal-faulting (Craig et al., 2014; Harada et al., 2013; Lay et al., 2013).
- ERF and MRF both show **two distinct pulses**, possibly representing the two events.



1. Key Points

1. Specific Intrinsic Mode Functions (IMFs) represent energy release at the earthquake source.
2. Energy Rate Functions (ERFs) generated from Hilbert spectral analysis of such IMF combinations.
3. Proposed ERFs match well with the Moment Rate Functions (MRFs) from teleseismic waveform modeling.
4. ERF-MRF match is controlled by the station azimuth and shaking intensity, and frequency and energy-based selection of IMFs.

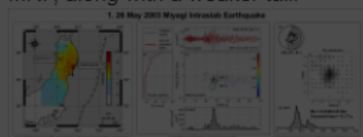
A short video explaining our work:

OPEN

5. Results

1. 26 May 2003 Miyagi Intraslab Earthquake (Mw 7.0, depth 67.0 km)

- Up-dip slip (towards east-northeast).
- Station AKTH16, WNW (305.98° azimuth), seismic intensity (SI) 4.
- Single, dominant, ~10 s energy pulse captured by both the ERF and MRF, along with a weaker tail.



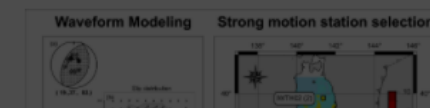
OPEN

4. Methodology

2. Moment Rate Function (MRF) generated from waveform modeling to validate the ERF algorithm.

Selection of strong-motion stations

1. Slip distribution, along with the seismic intensity distribution maps (JMA, 1996; ShakeMap, 2017), used to select stations within the inferred azimuthal range and seismic intensity > 3.



OPEN

6. Summary

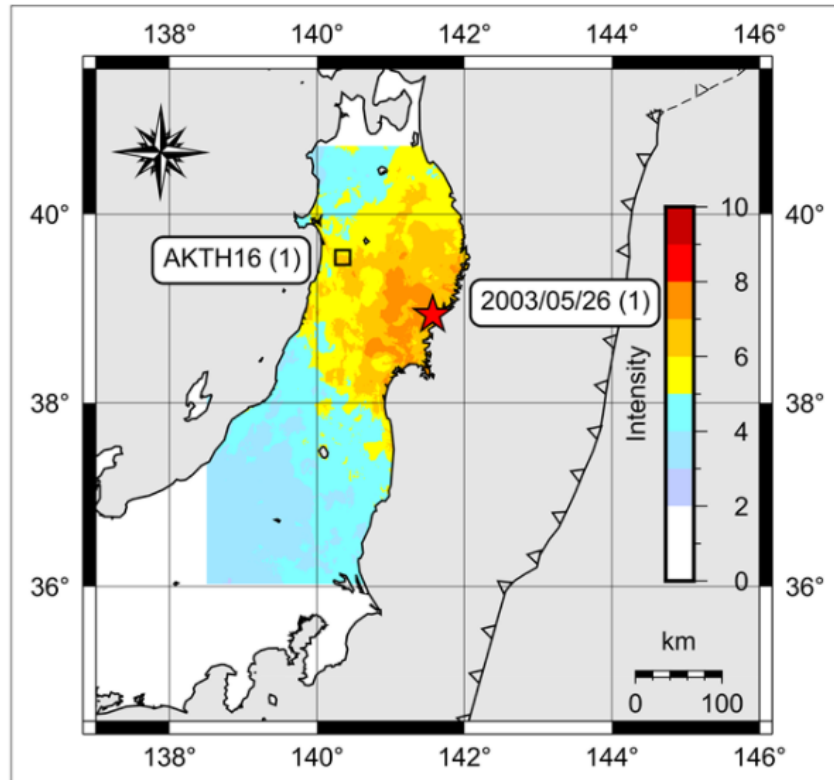
1. HHT-based ERF captures the **earthquake source energy release**, with a **higher resolution** offered by HHT as compared to Fourier analysis methods and wavelet transform.
2. ERF **retains frequency information**, is computationally faster for a rapid interpretation of an event, and **does not entail assumptions** of the fault geometry and velocity structure. These are clear advantages over the traditional MRF.
3. ERF captures **complex ruptures** (2005 Miyagi-Oki event) and sub-events or

OPEN

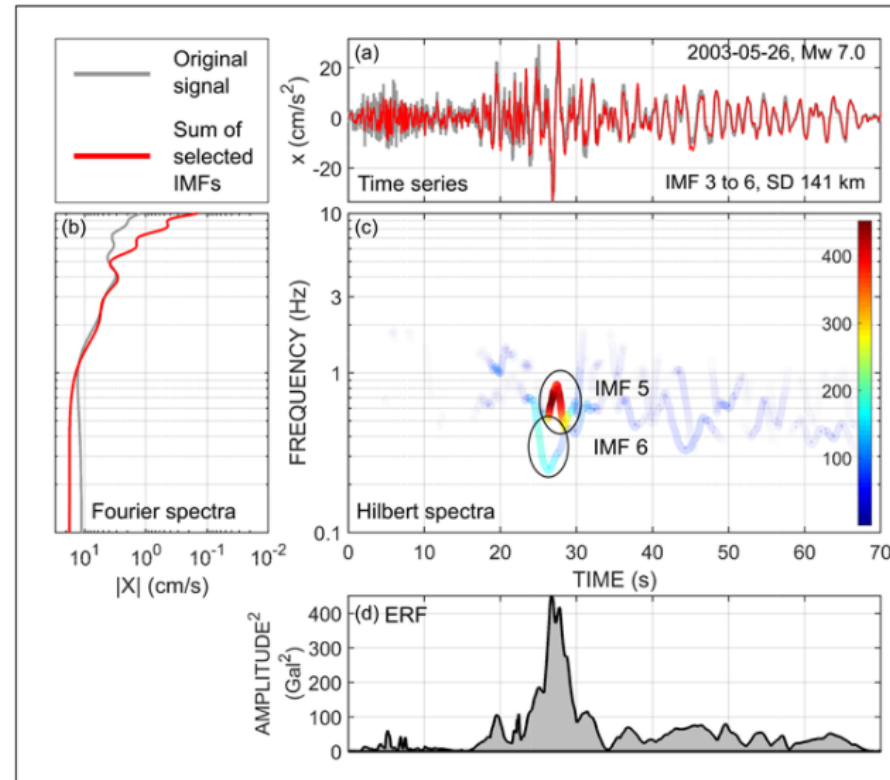
5. Results

1. 26 May 2003 Miyagi Intralab Earthquake (Mw 7.0).

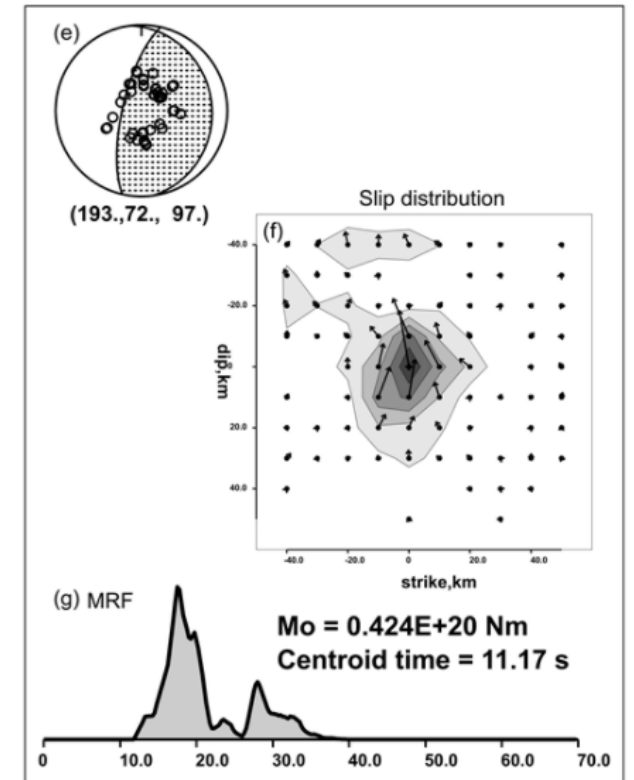
1. 26 May 2003 Miyagi Intralab Earthquake



1.1 Shakemap with epicenter (star) and station (square).



1.2 Strong motion analysis result.

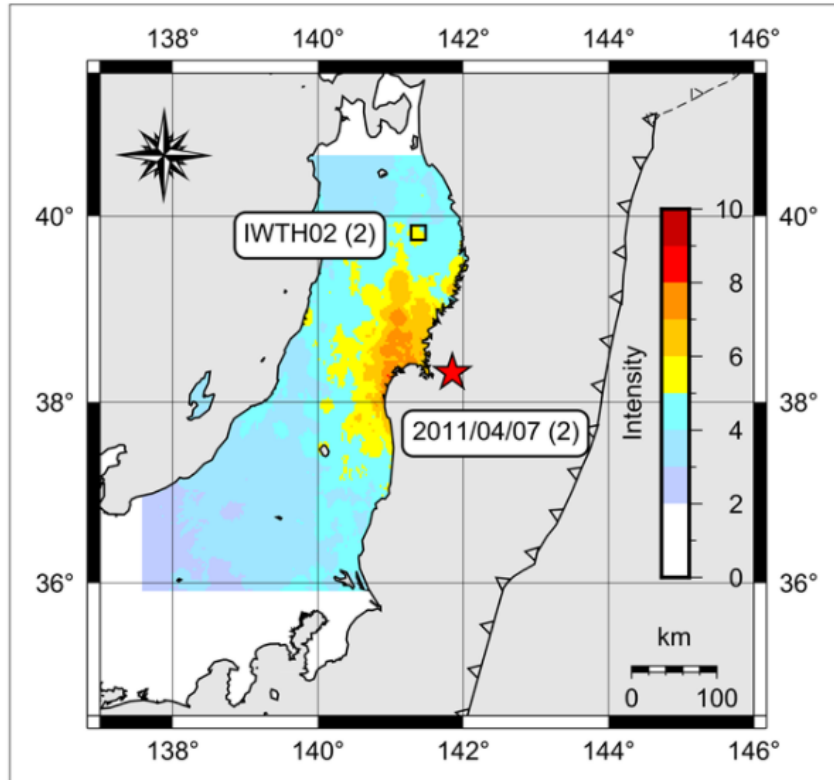


1.3 Teleseismic waveform modeling result.

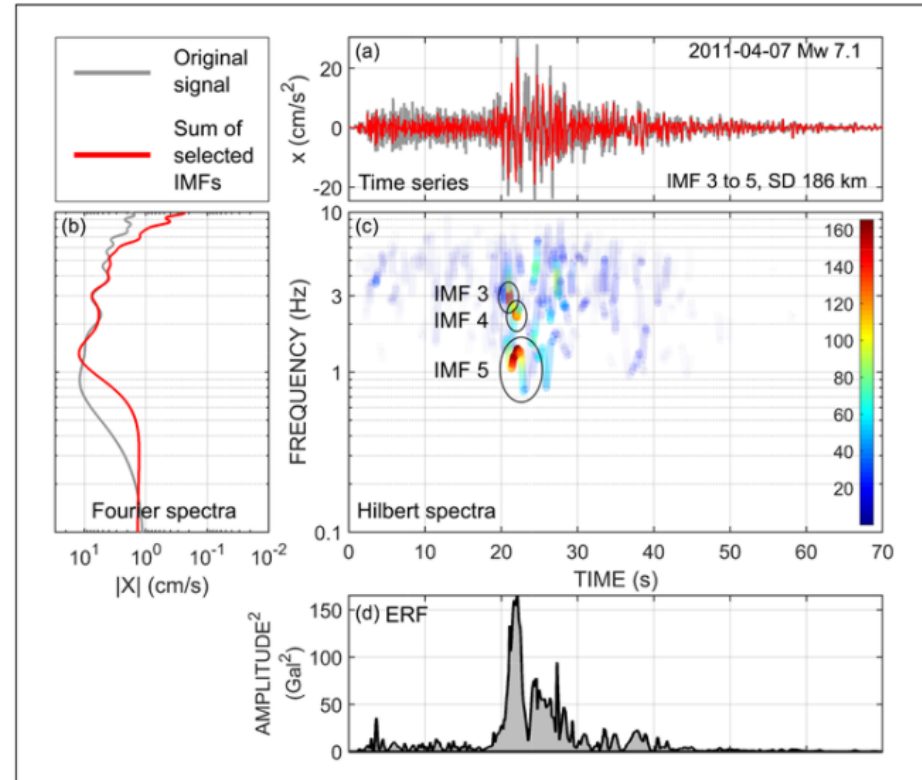
5. Results

1. 26 Mar 2003 Mivagi Intralab Earthquake (Mw 7.0).

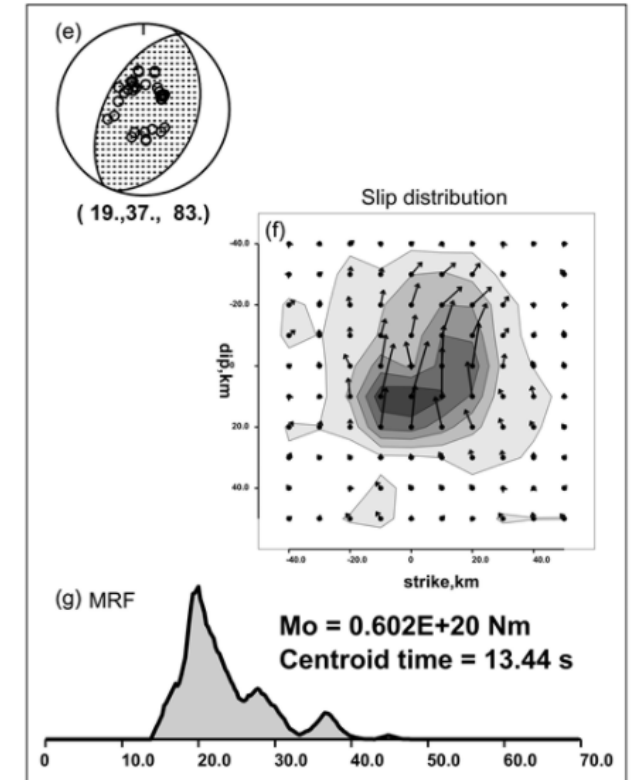
2. 07 April 2011 Miyagi Intralab Earthquake



2.1 Shakemap with epicenter (star) and station (square).



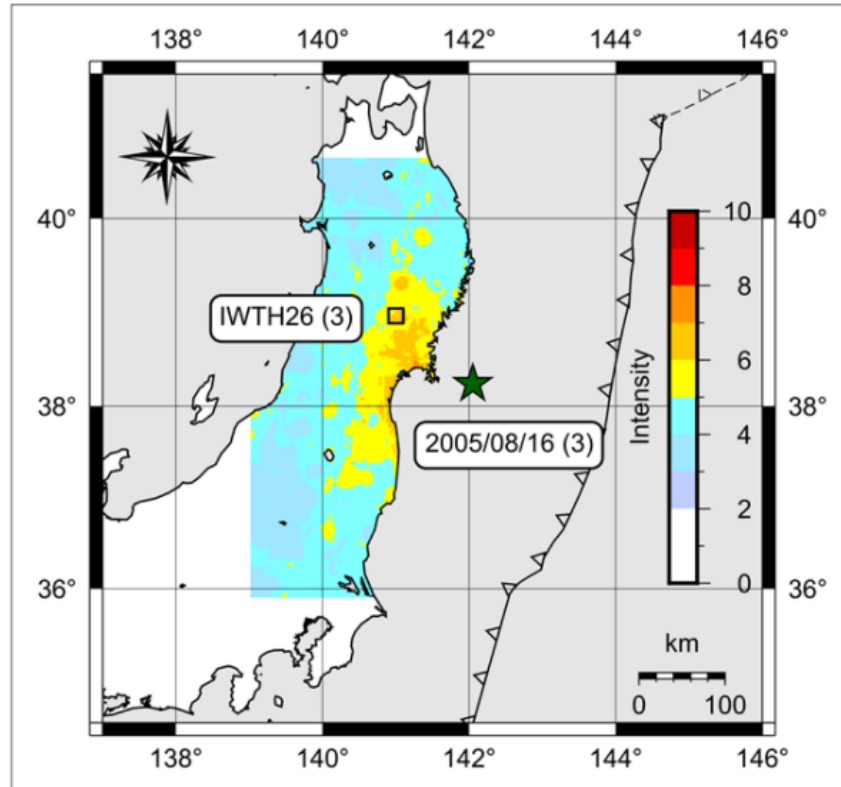
2.2 Strong motion analysis result.



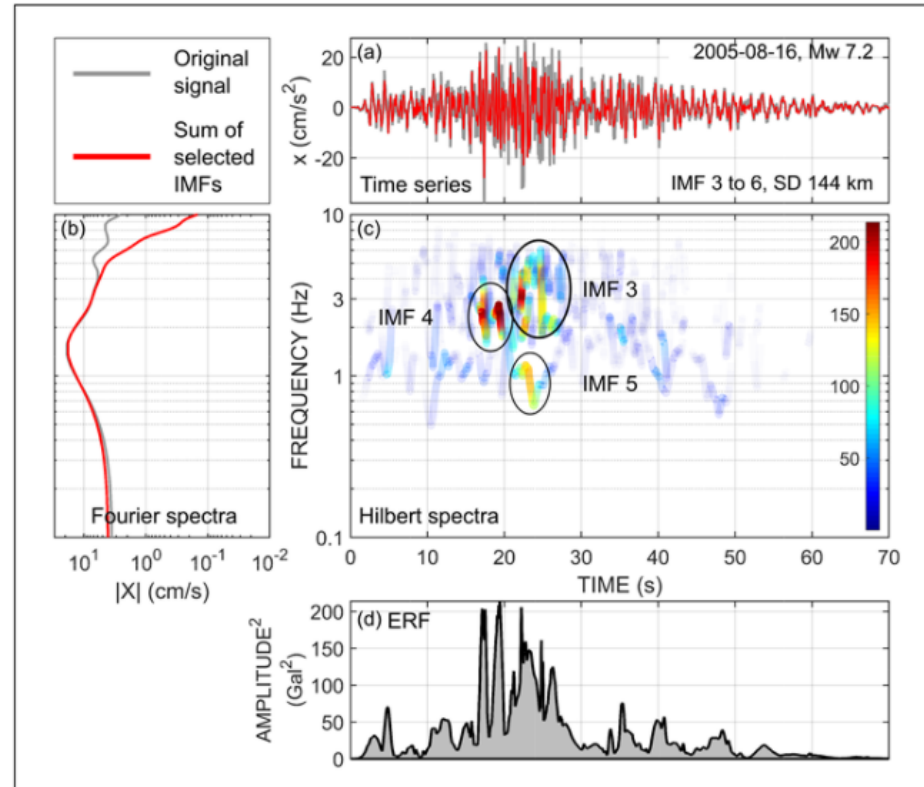
3.3 Teleseismic waveform modeling result.

5. Results

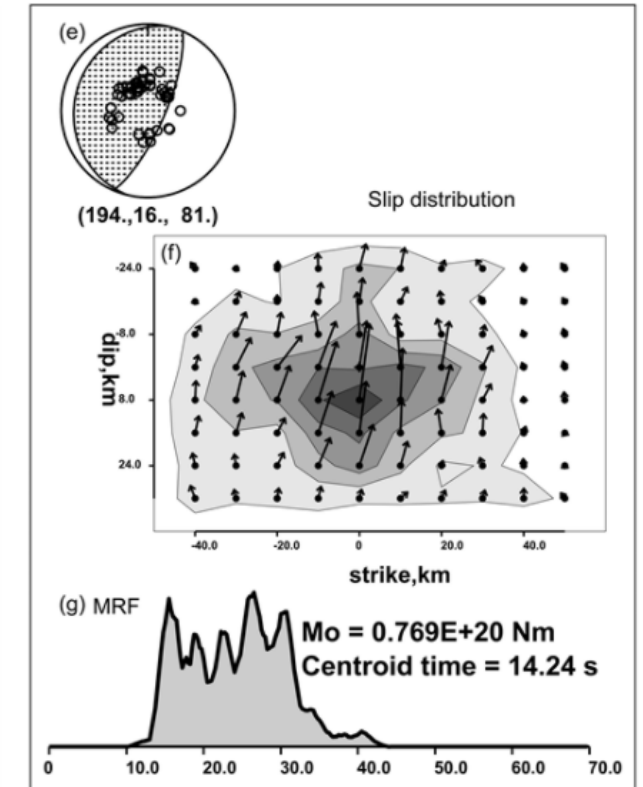
3. 16 August 2005 Miyagi-Oki Interplate Earthquake



3.1 Shakemap with epicenter (star) and station (square).



3.2 Strong motion analysis result.



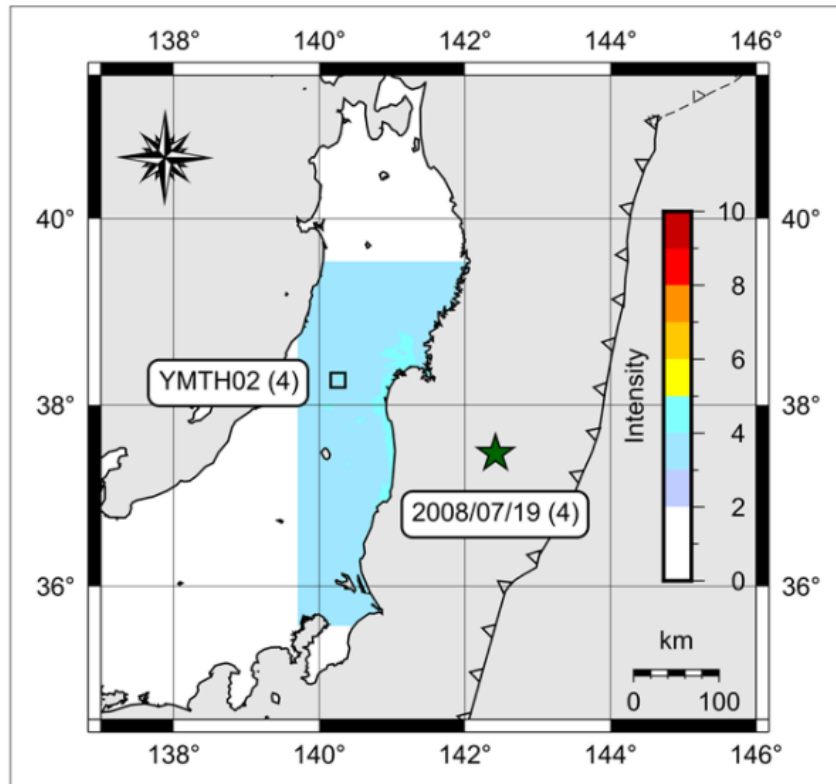
3.3 Teleseismic waveform modeling result.

5. Results

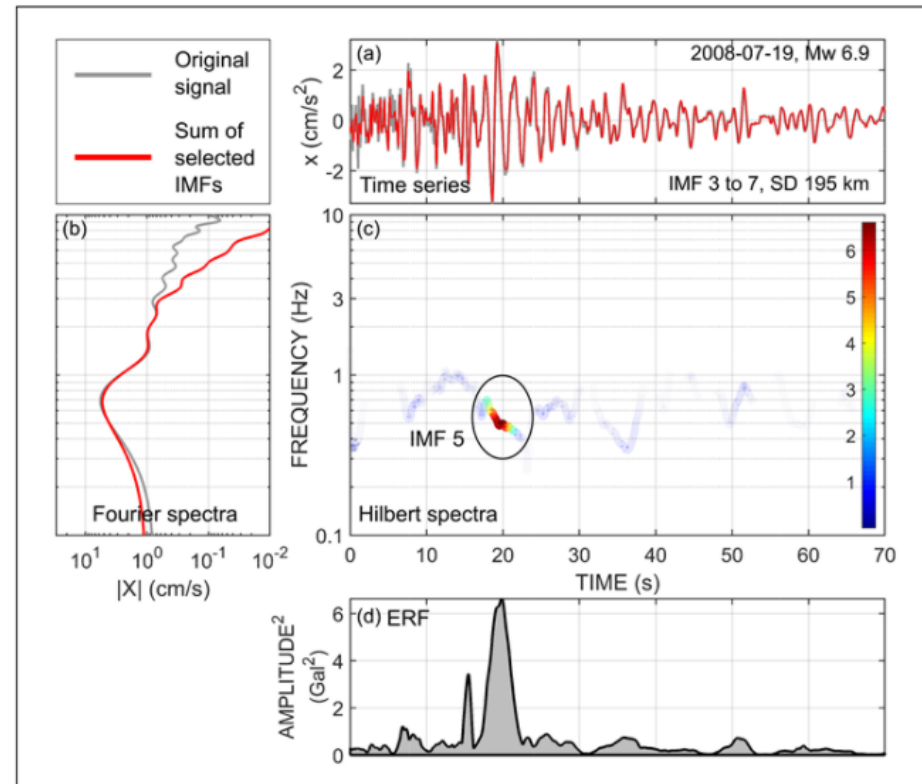
- A shallow interplate event; low-frequency energy

(Ye et al. 2013)

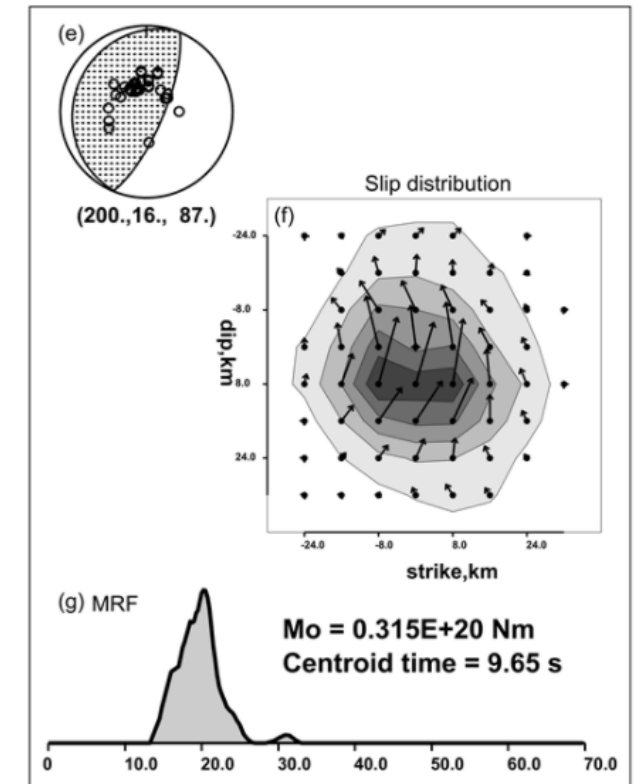
4. 19 July 2008 Fukushima-ken Oki Interplate Earthquake



4.1 Shakemap with epicenter (star) and station (square).



4.2 Strong motion analysis result.



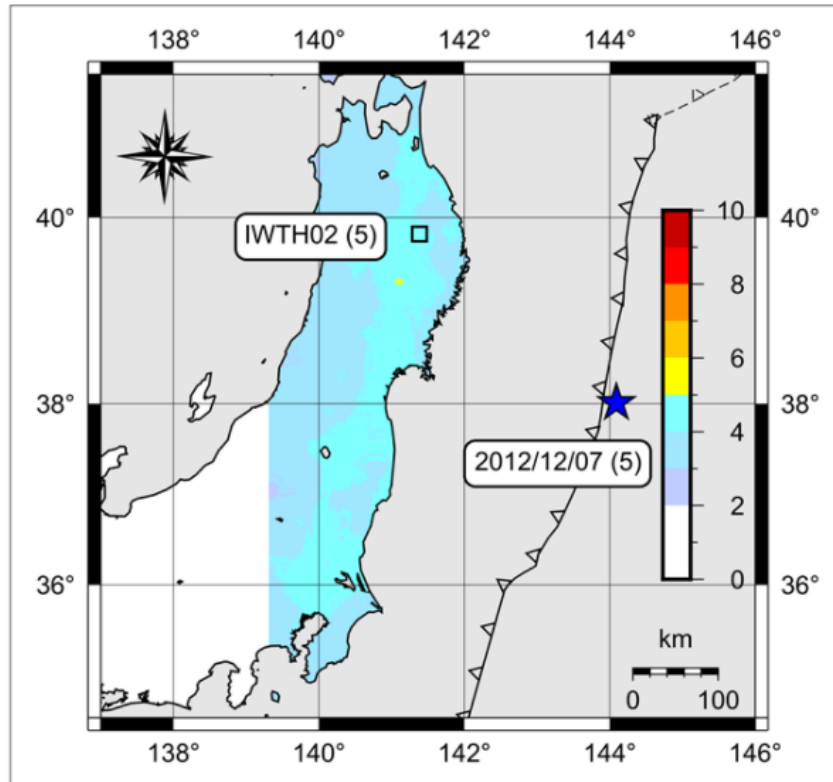
4.3 Teleseismic waveform modeling result.

5. Results

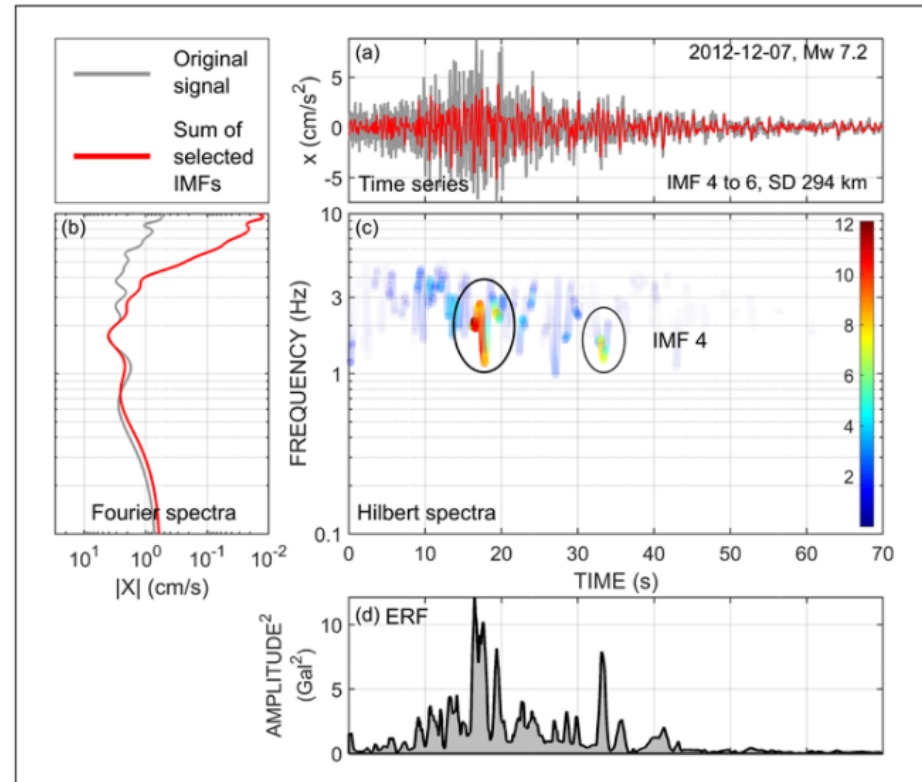
(Ye et al., 2013).

4. 19 July 2008 Fukushima-ken Oki Interplate Earthquake

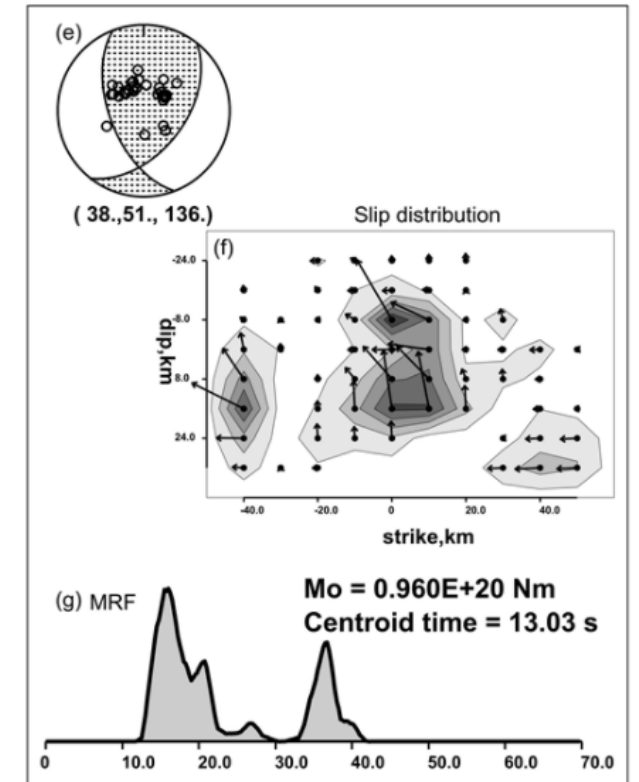
5. 07 December 2012 Kamaishi Intraplate Earthquake



5.1 Shakemap with epicenter (star) and station (square).



5.2 Strong motion analysis result.



5.3 Teleseismic waveform modeling result.

6. Summary

1. HHT-based **ERF captures the earthquake source energy release**, with a **higher resolution** offered by HHT as compared to Fourier analysis methods and wavelet transform.
2. **ERF retains frequency information**, is computationally faster for a rapid interpretation of an event, and **does not entail assumptions** of the fault geometry and velocity structure. These are clear advantages over the traditional MRF.
3. **ERF captures complex ruptures** (2005 Miyagi-Oki event) and sub-events or multiple independent events (2012 Kamaishi event).
4. **Improvement** in the criterion for the **selection of stations** based on their **azimuth**, inferred from the slip distribution. Strike of the Japan Trench provides an important starting point. Further, stations with **seismic intensity** > 3 provide optimal results.
5. **Improvement in the selection of IMF(s)**, based on a **frequency and energy** criterion corresponding with the bandpass filtering in waveform inversion.

1. Key Points

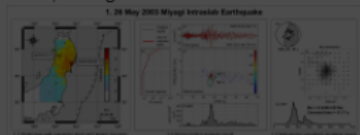
1. Specific Intrinsic Mode Functions (IMFs) represent energy release at the earthquake source.
2. Energy Rate Functions (ERFs) generated from Hilbert spectral analysis of such IMF combinations.
3. Proposed ERFs match well with the Moment Rate Functions (MRFs) from teleseismic waveform modeling.
4. ERF-MRF match is controlled by the station azimuth and shaking intensity, and frequency and energy-based selection of IMFs.

A short video explaining our work

OPEN

5. Results

1. **26 May 2003 Miyagi Intraslab Earthquake (Mw 7.0, depth 67.0 km)**
 - Up-dip slip (towards east-northeast).
 - Station AKTH16, WNW (305.98° azimuth), seismic intensity (SI) 4.
 - Single, dominant, ~10 s energy pulse captured by both the ERF and MRF, along with a weaker tail.



OPEN

4. Methodology

2. Moment Rate Function (MRF) generated from waveform modeling to validate the ERF algorithm.

Selection of strong-motion stations

1. Slip distribution, along with the seismic intensity distribution maps (JMA, 1996; ShakeMap, 2017), used to select stations within the inferred azimuthal range and seismic intensity > 3.



OPEN

6. Summary

1. HHT-based **ERF captures the earthquake source energy release**, with a **higher resolution** offered by HHT as compared to Fourier analysis methods and wavelet transform.
2. **ERF retains frequency information**, is computationally faster for a rapid interpretation of an event, and **does not entail assumptions** of the fault geometry and velocity structure. These are clear advantages over the traditional MRF.
3. **ERF captures complex ruptures** (2005 Miyagi-Oki event) and sub-events or

OPEN

Energy release patterns and shaking effects of earthquakes in the Japan Trench: A Hilbert-Huang Transform approach

*Swapnil Mache¹, Kusala Rajendran¹

1. Indian Institute of Science, Bangalore

Subduction zones showcase the multiplicity of earthquakes—interplate, intraplate and intraslab—with shallow, intermediate, or deep focus, associated with different energy release patterns and frequency contents. An understanding of the duration and frequencies associated with various pulses of energy is useful for damage assessment. Empirical Mode Decomposition (EMD) of strong-motion records and the application of Hilbert transform have been suggested to overcome the limitations of the Fourier spectral analysis in dealing with highly non-linear strong-motion records (Huang et al., 1998, Zhang et al., 2003). Following the same approach, we have been trying various methods of analysis using the KiK-net strong-motion records to explore the efficacy of these techniques in representing the source of the rupture, in terms of energy release and frequency distribution. Our previous studies used EMD and time-frequency analysis tools such as spectrogram, scalogram, and Hilbert spectrum, using Intrinsic Mode Functions (IMFs) of the original signals as inputs. Nishant (2019) made random picks of IMFs to represent sources by correlating the sum of the selected IMFs with the original signal but found that the results were station dependent. We selected IMFs based on their frequency content (0.1 to 3 Hz) and used their linear combinations to develop the Energy Release Functions (ERF) for individual earthquakes (Mache et al., 2019). They reported that the ability to capture the signature of the original signal using the IMFs varied between earthquakes and stations. Next, we selected stations based on the direction of rupture inferred from teleseismic waveform models. The use of appropriate combinations of individual IMFs, chosen based on the direction of slip, resulted in ERFs whose shapes compared better with the Moment Rate Functions (MRFs) obtained from the teleseismic models. To further explore the station dependence on the resolution of ERFs viz-a-viz the MRFs, we used the instrumental seismic intensity distribution maps (JMA 1996, Shabestari and Yamazaki 2001) to select the stations. We analyzed five earthquakes; two interplate (Mw 7.2 2005 Miyagi, and Mw 6.9 2008/07/19), two intraplate (Mw 7.0 2003 Sendai, and Mw 7.2 2012 Kamaishi) and one intraslab (Mw 7.1 2011 Miyagi), following the above methodologies. This abstract presents the initial results of our study, which to our knowledge, is the first of its kind and holds significant potential in understanding the spatial and temporal patterns of energy release and their associated frequencies.

On the use of IMFs based on their frequencies, we find that a linear combination of appropriate signals can lead to ERFs that compare well with their respective MRFs. The selection of stations in the direction of rupture generates better-resolved spectra. While using the seismic intensities, we find that for values three and higher, stations located along the direction of rupture propagation produce ERFs that correlate better with their respective MRFs, as observed for the 2011 Miyagi earthquake. The use of stations located along the direction of the trench also shows a good correlation. For seismic intensities lower than 3, there is a decay in the energy release and hence a poor reproduction of the ERFs. For complex ruptures (2003 Sendai, 2005 Miyagi, and 2012 Kamaishi), the ERFs are not smooth, with their energy distributed in bands of varying frequencies. It could be due to changes in slip direction or generation of sub-events, but the fact that the shapes of both the MRF and ERF are comparable adds credence to our analysis. We find that the local geology also plays an essential role in limiting the energy distribution within a frequency range, an issue that needs further exploration using more examples.

Keywords: strong-motion, spectral analysis, Hibert-Huang transform, energy release, Japan Trench, intraslab, intraplate, and interplate earthquakes